iScience

CellPress
OPEN ACCESS

Review

Structural characterization of the mitochondrial Ca^{2+} uniporter provides insights into Ca^{2+} uptake and regulation

Wenping Wu,[1,2] Jimin Zheng,[1,*] and Zongchao Jia[3,*]

SUMMARY

The mitochondrial uniporter is a Ca^{2+}-selective ion-conducting channel in the inner mitochondrial membrane that is involved in various cellular processes. The components of this uniporter, including the pore-forming membrane subunit MCU and the modulatory subunits MCUb, EMRE, MICU1, and MICU2, have been identified in recent years. Previously, extensive studies revealed various aspects of uniporter activities and proposed multiple regulatory models of mitochondrial Ca^{2+} uptake. Recently, the individual auxiliary components of the uniporter and its holocomplex have been structurally characterized, providing the first insight into the component structures and their spatial relationship within the context of the uniporter. Here, we review recent uniporter structural studies in an attempt to establish an architectural framework, elucidating the mechanism that governs mitochondrial Ca^{2+} uptake and regulation, and to address some apparent controversies. This information could facilitate further characterization of mitochondrial Ca^{2+} permeation and a better understanding of uniporter-related disease conditions.

INTRODUCTION

Calcium is a vital second messenger in cells and is involved in almost all fundamental functions of life. Intracellular Ca^{2+} homeostasis is the basis of normal physiological metabolism; excessive Ca^{2+} induces the production of reactive oxygen species (ROS) and the permeability transition of the inner mitochondrial membrane (IMM) to trigger apoptosis (Orrenius et al., 2003). Mitochondria are vital intracellular organelles that regulate the spatial and temporal profile of cellular Ca^{2+} signaling (Graier et al., 2007). Mitochondrial Ca^{2+} uptake is accomplished by a uniporter located in the IMM (Gunter and Pfeiffer, 1990; Kamer and Mootha, 2015; Kirichok et al., 2004; Marchi and Pinton, 2014; Mishra et al., 2017; Rizzuto et al., 2012) that participates in an array of cellular functions, including the maintenance of cellular Ca^{2+} homeostasis, modulation of cell death and survival, and stimulation of ATP production (Balaban, 2009; Denton, 2009; Duchen et al., 2008; Murgia and Rizzuto, 2015; Orrenius et al., 2003). The Ca^{2+} uptake process is driven by the potential difference across the IMM ($\Delta\psi_m$, −180 mV) generated by the respiratory chain (Drago et al., 2011; Nicholls, 2005; O'Rourke, 2007; Rizzuto et al., 2012). In contrast, mitochondrial Ca^{2+} efflux is achieved mainly via the Na^+/Ca^{2+} exchanger (NCLX), which mediates the exchange of 3 sodium ions per calcium ion (Crompton et al., 1977; Palty et al., 2004, 2010); the H^+/Ca^{2+} exchanger (LETM1), containing leucine zipper and EF-hand (EF-hand is calcium-binding motif that is defined by its helix-loop-helix secondary structure as well as the ligands presented by the loop to coordinate the Ca^{2+} ion. The designation "EF hand" is derived from the structural orientation of the two α-helices (E and F) that form together with the Ca^{2+}-binding loop of 12 residues the highly conserved metal-binding consensus sequence) domains (Jiang et al., 2009; Tsai et al., 2014); and the mitochondrial permeability transition pore (mPTP), which is associated with the physiological functions of respiration and metabolism (Barsukova et al., 2011; Elrod et al., 2010; Ichas et al., 1997; O-Uchi et al., 2014; Rasola and Bernardi, 2007).

The composition of uniporters has been identified over the past decade and includes the mitochondrial Ca^{2+} uniporter (MCU) (Baughman et al., 2011; De Stefani et al., 2011), MCU regulatory subunit b (MCUb) (Raffaello et al., 2013), essential MCU regulator (EMRE) (Sancak et al., 2013), and the mitochondrial Ca^{2+} uniporter protein 1/2 (MICU1 and MICU2) (Perocchi et al., 2010; Plovanich et al., 2013). MICU1 was the first component identified through comparative physiology, evolutionary genomics, and organelle proteomics

[1]College of Chemistry, Beijing Normal University, Beijing 100875, China

[2]School of Medicine, Hangzhou Normal University, Hangzhou, Zhejiang 311121, China

[3]Department of Biomedical and Molecular Sciences, Queen's University, Kingston, ON K7L 3N6, Canada

*Correspondence: jimin_z@bnu.edu.cn (J.Z.), jia@queensu.ca (Z.J.)

https://doi.org/10.1016/j.isci.2021.102895

approaches; this protein resides in the mitochondrial intermembrane space (IMS) and contains two canonical EF-hands (Perocchi et al., 2010) (Csordas et al., 2013; Mallilankaraman et al., 2012b). MCU is the core transmembrane subunit of the uniporter and can self-assemble to form an oligomeric pore structure for the transport of Ca^{2+} from the IMS to the matrix (Chaudhuri et al., 2013; Martell et al., 2012; Raffaello et al., 2013). MCUb, a paralog of MCU, negatively regulates the Ca^{2+} uptake of the uniporter (Lambert et al., 2019; Raffaello et al., 2013). EMRE is a metazoan-specific single transmembrane protein required for the basal activity of the metazoan uniporter that can mediate the interaction between MICU1 and MCU (Sancak et al., 2013; Tsai et al., 2016). Most interestingly, EMRE orthologs have been identified in chytrid fungi; these orthologs regulate MCU activity in a manner similar to EMRE in metazoans (Pittis et al., 2020). MICU2 is a homolog of MICU1 and possesses two canonical EF-hands involved in modulating mitochondrial Ca^{2+} permeation in an MICU1-dependent manner (Kamer and Mootha, 2014; Patron et al., 2014; Plovanich et al., 2013). MICU3 is another paralog of MICU1 that is specifically expressed in the central nervous system (CNS) (Patron et al., 2019; Plovanich et al., 2013). MICU3 tunes the Ca^{2+} sensitivity of the MCU to facilitate mitochondrial Ca^{2+} uptake in axons, which contributes to accelerated ATP production to sustain the intricate metabolic function of neuronal cells (Ashrafi et al., 2020). In addition, mitochondrial calcium uniporter regulator 1 (MCUR1) was originally identified as an essential uniporter component that modulates uniporter Ca^{2+} uptake by interacting with MCU (Mallilankaraman et al., 2012a). Its ablation abrogates mitochondrial Ca^{2+} uptake, disrupts oxidative phosphorylation, and decreases the production of ATP to trigger autophagy (Mallilankaraman et al., 2012a). However, subsequent research clarified that MCUR1 does not directly regulate MCU; instead, mitochondrial membrane potential is impaired under the suppressive effects of MCUR1 (Paupe et al., 2015).

The cytosolic Ca^{2+} concentration ($[Ca^{2+}]_c$) must reach a high level (~5–10 μM) to stimulate mitochondrial Ca^{2+} uptake, a requirement that is believed to be due to the low inherent Ca^{2+} affinity (K_d ~20–30 μM) of the uniporter, which inhibits Ca^{2+} conduction under resting conditions (Marchi and Pinton, 2014). The existence of microdomains linking mitochondria with the ER offers a spatial basis for the aforementioned theory, given that the $[Ca^{2+}]$ of microdomains can transiently reach a high level upon stimulation (Patergnani et al., 2011; Rizzuto et al., 1998). However, electrophysiological experiments in mitoplasts have indicated that the selectivity filter of the uniporter has an extremely high Ca^{2+} affinity with a $K_d \leq 2$ nM and high Ca^{2+} selectivity (Kirichok et al., 2004), but mitochondrial Ca^{2+} uptake can be independent of basal cytosolic fluctuations ($[Ca^{2+}]_c$~100 nM) (Csordas et al., 1999, 2010; Giacomello et al., 2010). This apparent contradiction implies the existence of tight regulation by auxiliary subunits (e.g., MICU1, MICU2, EMRE, etc.) in the Ca^{2+} uptake process, but this issue remains an important open question (Boyman and Lederer, 2020).

To date, numerous functional studies have documented that MICU1 and MICU2 modulate the process of Ca^{2+} permeation as gatekeepers. We summarize three representative regulatory models: (i) MICU2 inhibits the channel under basal conditions as a negative regulator, and MICU1 cooperatively activates the MCU pore at a high $[Ca^{2+}]_c$ (Patron et al., 2014). MICU1 and MICU2 perform opposite functions in regulating MCU activity and cooperate to fine-tune the mitochondrial Ca^{2+} uptake (Patron et al., 2014). (ii) The MICU1 and MICU2 of the heterodimer set the threshold collectively to regulate Ca^{2+} uptake through their individual and nonredundant functions. MICU1 can act independently as a gatekeeper, but the role of MICU2 requires MICU1 (Kamer and Mootha, 2014). (iii) MICU1 mediates the gatekeeping and cooperative activation of MCU independently, whereas MICU2 increases the threshold set by MICU1 and reduces the $[Ca^{2+}]$ sensitivity for the cooperative activation of MCU (Payne et al., 2017). Additionally, the coordination of 3 or 4 Ca^{2+} ions by EF-hands is a prerequisite for triggering mitochondrial Ca^{2+} uptake (Payne et al., 2017). These three regulatory models can be largely unified using an essential principle, i.e., the inhibition and activation functions of MICU1 and MICU2 correspond to the *apo* and *holo* states of their EF-hands. Thus, Ca^{2+} seems to be the crucial "key" to open the EF-hand "lock" of the MICU1-MICU2 gatekeeper and activate the ion channel.

Over the past decade, extensive uniporter functional studies have been reported, illuminating different aspects of mitochondrial Ca^{2+} uptake. Our understanding of uniporter function and regulation has been greatly augmented by recent structural studies of uniporters. These structures provided considerable insight into the mechanism underlying Ca^{2+} uptake and regulation. In this review article, we focus on the structures of the uniporter and related components to examine the regulatory mechanism underlying mitochondrial Ca^{2+} uptake, and we outline unanswered questions for future study.

STRUCTURAL CHARACTERISTICS OF UNIPORTER COMPONENTS

MCU structures in various species

MCU is the core subunit and performs the pivotal function of directly transporting Ca^{2+} from the IMS to the mitochondrial matrix, but its indiscernible sequence homology to the canonical calcium channel makes its structure difficult to model (Bick et al., 2012). However, genome sequence analyses have demonstrated that MCU homologs in many fungal lineages are the exclusive component of the uniporter, defining the minimal genetic component for mitochondrial Ca^{2+} uptake (Bick et al., 2012; Kamer and Mootha, 2015; Kovacs-Bogdan et al., 2014). In some nonmetazoans, such as trypanosomes, the uniporter is composed of MCU, MCUb, MICU1, and MICU2 but lacks EMRE and MCUR1 orthologs and is thus simpler than that of mammalian cells (Docampo et al., 2014; Lander et al., 2018). Thus, MCU orthologs of nonmetazoans represent a simplified system ideal for initial structural investigations, which enticed structural biologists to focus on fungal MCU structures. In 2018, publications reported four fungal MCU structures that were determined by single-particle cryo-electron microscopy (cryo-EM) or X-ray crystallography techniques in a resolution range of 3.1-3.8 Å (Baradaran et al., 2018; Fan et al., 2018; Nguyen et al., 2018; Yoo et al., 2018). Undoubtedly, the solution of these structures not only provided insights into MCU architecture but also marked an epoch in uniporter structure research. All four MCU homolog structures feature homotetramers with almost indistinguishable conformations, highlighting their structural conservation (Figures 1A and 1B). Each protomer is segmented into three structural domains, namely, the N-terminal domain (NTD), coiled-coil domain (CCD), and transmembrane domain (TMD) (Figures 1A and 1B) (Baradaran et al., 2018; Fan et al., 2018; Nguyen et al., 2018; Yoo et al., 2018). Interestingly, fungal MCU structures show a symmetry mismatch between TMDs and NTDs in which TMDs have a tetrameric configuration, while NTDs exhibit approximately twofold rotational symmetry.

An MCU construct with deletion of the NTD (cMCU-ΔNTD) from *Caenorhabditis elegans* was the first structure determined using a combination of nuclear magnetic resonance (NMR) and electron microscopy (EM) tools and features a special bistratal pentameric architecture (Oxenoid et al., 2016). The structure of the pentameric calcium channel provided both the first insight into the architecture of MCU and a structural basis for subsequent investigations. The intact tetrameric structures of fungal MCUs represent the opening conformation of the channel that can transport Ca^{2+} independent of other auxiliary subunits, whereas the cMCU structure exhibits a closed state with the bottom section blocked, likely due to the absence of EMRE (Oxenoid et al., 2016). These different assembly patterns should not be attributed to fungi and metazoans of different species or to the NTD deletion. The pentameric architecture has not been observed in subsequently determined metazoan MCU structures, even in the MCU-ΔNTD from *Homo sapiens* and *Tribolium castaneum,* which feature the tetrameric configuration (Baradaran et al., 2018; Wang et al., 2019, 2020a). Thus, the peculiar pentameric organization of cMCU-ΔNTD currently stands as an "oddball." Generally, NMR spectroscopy is suitable for the structural determination of low-molecular-weight proteins, but some large membrane protein structures have been successfully solved using NMR (Hiller and Wagner, 2009; Huang and Kalodimos, 2017; Popovych et al., 2009; Tugarinov et al., 2005; Tzeng et al., 2012). Therefore, it is difficult to determine whether the discrepancy is caused by species specificity or different analytical techniques; an additional high-resolution *C. elegans* MCU structure is needed to solve this riddle. Multiple MCU structures from different species have revealed highly similar Ca^{2+} selectivity mechanisms but variations in species-specific architectural arrangements, demonstrating both evolutionary conservation and structural variability. Collectively, these MCU structures have paved the way for understanding the structural basis of Ca^{2+} transport and regulation. Given the structural complexity of the mitochondrial Ca^{2+} uptake system, in the following sections, we use the "divide and conquer" approach and discuss the NTD and Ca^{2+} conduction domain in detail.

NTDs of MCUs

The NTD has been documented to specifically modulate MCU Ca^{2+} uptake from the mitochondrial matrix and to act as a bridge connecting other subunits, such as MCUR1; however, the functional implications of MCU-MCUR1 remain to be elucidated (Lee et al., 2015, 2016; Tomar et al., 2016). Significant discrepancies exist in the structural assembly of NTDs between fungi and metazoans (Baradaran et al., 2018; Fan et al., 2018; Nguyen et al., 2018; Wang et al., 2019; Yoo et al., 2018). The fungal NTD assembles in a dimer-of-dimers configuration with two interfaces, whereas the human (or *zebrafish*) NTD adopts a side-by-side packing mode around the channel side similar to a crescent moon (Figures 1C and 1D), which completely perturbs the symmetry of the Ca^{2+} channel (Baradaran et al., 2018; Fan et al., 2018; Nguyen et al., 2018; Yoo et al., 2018). Strikingly, the new assembly pattern creates conditions favorable for channel dimerization by NTDs mediated via abundant hydrogen bonding interactions (Figure 1C) (Wang et al., 2019). Moreover, this pattern can strengthen the communication of two channels, which probably enhances the efficiency

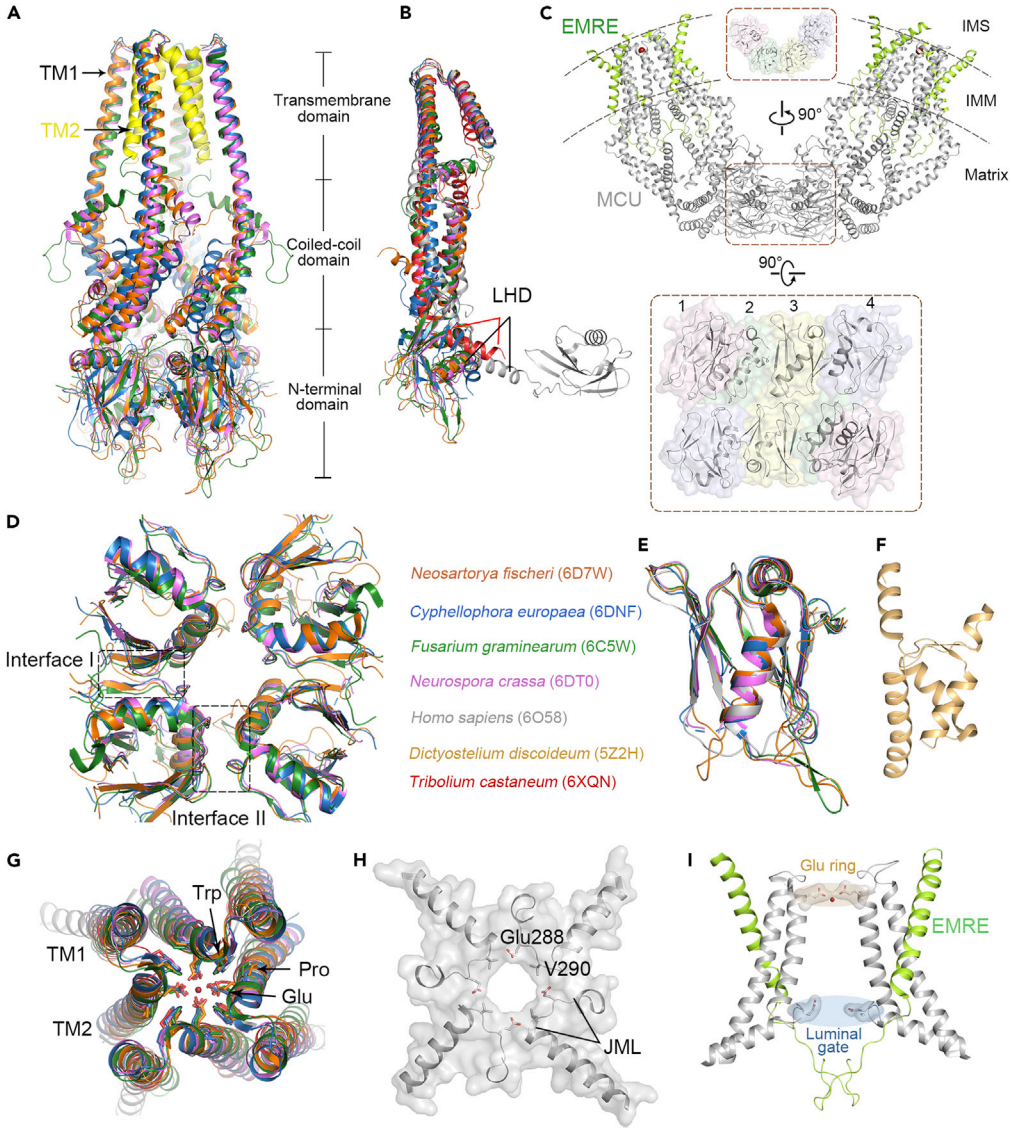

Figure 1. Structures of mitochondrial Ca^{2+} uniporters from various species

(A) Structural alignment of MCU tetramers from various fungi. Fungal MCU structures feature a transmembrane domain (TMD), coiled-coil domain (CCD), and N-terminal domain (NTD). Yellow ribbons represent the ion permeation channel.

(B) Structural alignment of MCU protomers from various species. Metazoan MCUs possess extra linker helix domains (LHDs).

(C) Side view of the overall human MCU-EMRE dimeric structure. Insets show the side and top views of NTDs in the human MCU-EMRE complex.

(D) Structural alignment of the NTDs of MCUs from various fungi. The intermolecular interaction interfaces are indicated by dotted boxes.

(E) Structural alignment of NTD protomers of MCUs from various species.

(F) Ribbon diagram of a DdNTD protomer.

(G) Structural alignment of Ca^{2+} selectivity filters viewed from the top. The curial residues are shown in stick representation. Ca^{2+} ion is presented as a red sphere.

(H) Top view of the surface-rendered JML (luminal gate). The curial residues are shown in stick representation.

(I) The two Ca^{2+} conduction pathway gates (Glu ring and luminal gates) in human MCU. The curial residues are shown in stick representation. Ca^{2+} ion is presented as a red sphere.

of Ca^{2+} transport and reduces the response time upon stimulation. Despite the low sequence identity, NTD protomers feature analogous structural folding containing abundant β-strands across species (Figure 1E), except in the *Dictyostelium discoideum* (Dd) NTD structure, which instead features abundant α-helices that could represent a different and yet unknown regulatory mechanism (Figure 1F) (Baradaran et al., 2018; Fan et al., 2018; Lee et al., 2015, 2016; Nguyen et al., 2018; Wang et al., 2019; Yoo et al., 2018; Yuan et al., 2020). Therefore, NTDs exhibit considerable structural variability, probably due to the diverse modulatory mechanisms of the mitochondrial matrix in different species to adapt to varying physiological environments.

The NTD contains a negatively charged domain that can bind divalent cations with millimolar affinity, which is considered to destabilize the self-assembly equilibrium (oligomers and monomers) and disrupt uniporter activity (Lee et al., 2016). The switch between oligomeric and monomeric NTDs reveals a potential negative feedback modulation mechanism in which a high $[Ca^{2+}]_m$ inhibits MCU activity owing to the destabilization of self-association (Lee et al., 2016; Yuan et al., 2020). Interestingly, the negatively charged patch was subsequently identified as a matrix Ca^{2+} inhibition sensor that can even override the MICU1-MICU2-dependent activation of MCU under Ca^{2+}-binding conditions when this sensor is occupied (Vais et al., 2020). In contrast, matrix negative feedback modulation strictly depends on the association between MICU1-MICU2 and the channel, demonstrating the coupled Ca^{2+}-regulated mechanisms inside and outside the IMM (Vais et al., 2020). However, how the NTD contributes to Ca^{2+} uptake remains controversial. Rescuing NTD-deficient MCU in MCU-silenced cells had a somewhat negative impact on mitochondrial Ca^{2+} uptake, likely as a result of the destabilization of MCU self-assembly (Lee et al., 2015, 2016). In contrast, this functional deficiency was not observed in a Ca^{2+} clearance experiment in permeabilized cells in which the MCU_ΔNTD mutation did not impair the function of mitochondrial Ca^{2+} uptake (Oxenoid et al., 2016; Wang et al., 2019). This discrepancy is likely attributable to differences in cell lines, experimental methods, or detection sensitivity. Given that NTD deficiency destabilizes the dimerization of channels, it may influence the distribution of MCU on the IMM under resting conditions or on the inner boundary membrane (IBM) upon stimulation (Gottschalk et al., 2019). In addition, the NTD acts as a mitochondrial matrix redox sensor to regulate mitochondrial morphology and the MCU oligomerization state (Dong et al., 2017). These various roles emphasize the significance of the NTD in modulating physiological functions.

Core ion-conducting domains of MCUs

The ion-conducting domain resembles a truncated pyramid with bistratal transmembrane sections that modulates the transport of Ca^{2+} across the IMM (Baradaran et al., 2018; Fan et al., 2018; Nguyen et al., 2018; Wang et al., 2019, 2020a; Yoo et al., 2018). This domain comprises a highly conserved DIME motif (DIME motif is a conserved short stretch that linked the two transmembrane helices of MCU to face the intermembrane space), two transmembrane helices (TM1 and TM2), and a CCD with an internal hydrophilic ion cavity (Figure 1A). TM2 is located inside the channel and mediates the formation of tetrameric ion conduction pores, whereas TM1 embraces the periphery of the channel embedded in the membrane (Figure 1G) (Baradaran et al., 2018; Fan et al., 2018; Nguyen et al., 2018; Wang et al., 2019, 2020a; Yoo et al., 2018). The DIME motif resides on the neck of the channel and sharply narrows the Ca^{2+} channel, resulting in an hourglass shape. The DIME motif possesses two carboxylate rings that are crucial for mitochondrial Ca^{2+} uptake. A Glu ring with a narrow radius forms a selective filter for specific Ca^{2+} coordination, while an Asp ring with a large radius provides an acidic environment for recruiting Ca^{2+} to augment the efficiency of Ca^{2+} conduction (Figures 1G and Table 1) (Baradaran et al., 2018; Fan et al., 2018; Nguyen et al., 2018; Wang et al., 2019, 2020a; Yoo et al., 2018). This appropriate size of the MCU entrance in an acidic environment also provides a suitable binding pocket for the inhibitor. The most potent inhibitor of the uniporter, Ru360, was found to bind the Asp ring and adjacent serine, blocking the entrance of the ion pore (Cao et al., 2017); however, MICU1 decreased the Ru360 sensitivity of the uniporter by competing with the inhibitor for binding MCU (Paillard et al., 2018). Furthermore, the conserved rigid residues close to the DIME motif stabilize the proper configuration of the Ca^{2+} filter via close stacking interactions, rigidifying the side chain conformation of Glu via hydrogen bonds (Figure 1G) (Baradaran et al., 2018; Fan et al., 2018; Nguyen et al., 2018; Wang et al., 2019, 2020a; Yoo et al., 2018). The strictly conserved structures of the Ca^{2+} selectivity filter in various species demonstrate the uniform mechanism of Ca^{2+} permeation and provide structural safeguards for Ca^{2+} selection.

Additionally, human MCU contains a distinctive luminal gate mediated by a juxtamembrane loop (JML) at the exit of the transmembrane channel that performs a gating function to modulate Ca^{2+} release into the mitochondrial matrix (Figure 1H) (Wang et al., 2019). Intriguingly, this motif is disordered in fungal MCU structures and forms a considerably wider gate in beetle MCU, which may imply that this species does

Table 1. Structural data of the mitochondrial Ca^{2+} uniporter

PDB	Species	Components	Methods	Configurations	Asp ring radius (Å)	Glu ring radius (Å)	Resolution (Å)	References
5ID3	*C. elegans*	MCU	NMR, EM	Pentamer	~1.9	~3.0	–	(Oxenoid et al., 2016)
6C5W	*Ma*	MCU	X-ray	Tetramer	~4.0	~2.5	3.1	(Fan et al., 2018)
6D7W	*Nf*	MCU	Cryo-EM	Tetramer	~4.0	~2.25	3.8	(Nguyen et al., 2018)
6DT0	*Nc*	MCU	Cryo-EM	Tetramer	~4.4	~2.4	3.7	(Yoo et al., 2018)
6DNF	*C. europaea*	MCU	Cryo-EM	Tetramer	~3.9	~2.4	3.2	(Baradaran et al., 2018)
6O58	*Hs*	MCU, EMRE	Cryo-EM	Tetramer	~3.0	~2.0	3.6	(Wang et al., 2019)
6X4S	*Tc*	MCU, EMRE	Cryo-EM	Tetramer	~4.5	~2.0	3.5	(Wang et al., 2020a)
6WDN	*Hs*	MCU, EMRE, MICU1, MICU2	Cryo-EM	Tetramer	~3.2	~1.9	3.3	(Fan et al., 2020)
6WDO	*Hs*	MCU, EMRE, MICU1, MICU2	Cryo-EM	Tetramer	~3.1	~1.6	3.6	(Fan et al., 2020)
6XQN	*Tc, Hs*	MCU, EMRE, MICU1, MICU2	Cryo-EM	Tetramer	~4.5	~2.0	3.3	(Wang et al., 2020b)
6XJV	*Hs*	MCU, EMRE, MICU1, MICU2	Cryo-EM	Tetramer	~3.5	~1.6	4.2	(Wang et al., 2020c)
6XJX	*Hs*	MCU, EMRE, MICU1, MICU2	Cryo-EM	Tetramer	~3.5	~1.5	4.6	(Wang et al., 2020c)
6K7Y	*Hs*	MCU, EMRE, MICU1, MICU2	Cryo-EM	Tetramer	~4.5	~1.8	3.6	(Zhuo et al., 2020)

Abbreviations: PDB, Protein DataBank; C. elegans, *Caenorhabditis elegans*; Ma, *Metarhizium acridum*; Nf, *Neosartorya fischeri*; Nc, *Neurospora crassa*; Ce, *Cyphellophora europaea*; Hs, *Homo sapiens*; Ts, *Tribolium castaneum*; NMR, nuclear magnetic resonance; Cryo-EM, cryo-electron microscopy; X-ray, X-ray crystallography.

not need constricted gate regulation (Wang et al., 2020a). Human MCU contains two Ca^{2+} gates, i.e., a Glu ring gate to selectively filter Ca^{2+} and another gate serving as a luminal gate to ensure efficient Ca^{2+} permeation (Figure 1I) (Wang et al., 2019). In addition, metazoan MCU contains a linker helix domain (LHD) (Figure 1B), which is arranged to form a flat bottom and terminate the soluble ion cavity (Wang et al., 2019). This domain is also considered the "watershed" of the channel symmetry and asymmetry and breaks the uniform configuration of the entire MCU. The specificity of LHD offers a flexible transition for NTD side-by-side assembly and increases the conformational plasticity for channel dimerization. In addition to possessing multiple auxiliary subunits, metazoan MCUs display intricate structural details that imply more elaborate physiological regulation, including fundamental energy provision, aerobic metabolism, and abundant signal pathways. Obviously, crucial physiological functions must depend on and be supported by the sophisticated mechanism of mitochondrial Ca^{2+} uptake.

Structures of MICUs

MICU1 and/or MICU2 can inhibit MCU under resting conditions as gatekeepers and relieve inhibition with increased $[Ca^{2+}]_c$ (Ahuja and Muallem, 2014; Csordas et al., 2013; Foskett and Madesh, 2014; Kamer et al., 2017; Kamer and Mootha, 2014; Mallilankaraman et al., 2012b; Patron et al., 2014; Vecellio Reane et al., 2016). Their gatekeeping activity effectively suppresses excessive Ca^{2+} in the mitochondrial matrix to prevent ROS overload and protect cells against apoptosis. Thus, analyses of their structures are anticipated to expand our understanding of regulatory mechanisms. MICU1 structures were determined by crystallography at resolutions of 3.2 and 2.7 Å in the *apo* and *holo* states, respectively (Wang et al., 2014) (Figure 2A). The Ca^{2+}-free MICU1 structure forms a hexamer packed as a trimer of dimers with the C-helixes bundled together. In the presence of Ca^{2+}, the hexamer MICU1 transforms into multiple oligomers (Wang et al., 2014). In the trimer of dimers, MICU1 homodimers pack in an antiparallel mode with face-to-face configurations but feature entirely different interaction patterns and buried areas in Ca^{2+}-free and Ca^{2+}-bound states (Wang et al., 2014) (Figure 2A). The Ca^{2+}-free MICU1 homodimer features abundant electrostatic interactions with a large buried area, resulting in a tight homodimer, whereas the Ca^{2+}-bound structure features strong hydrophobic interactions with a small buried area, resulting in a loose homodimer (Wang et al., 2014) (Figure 2A). C-helixes contribute to

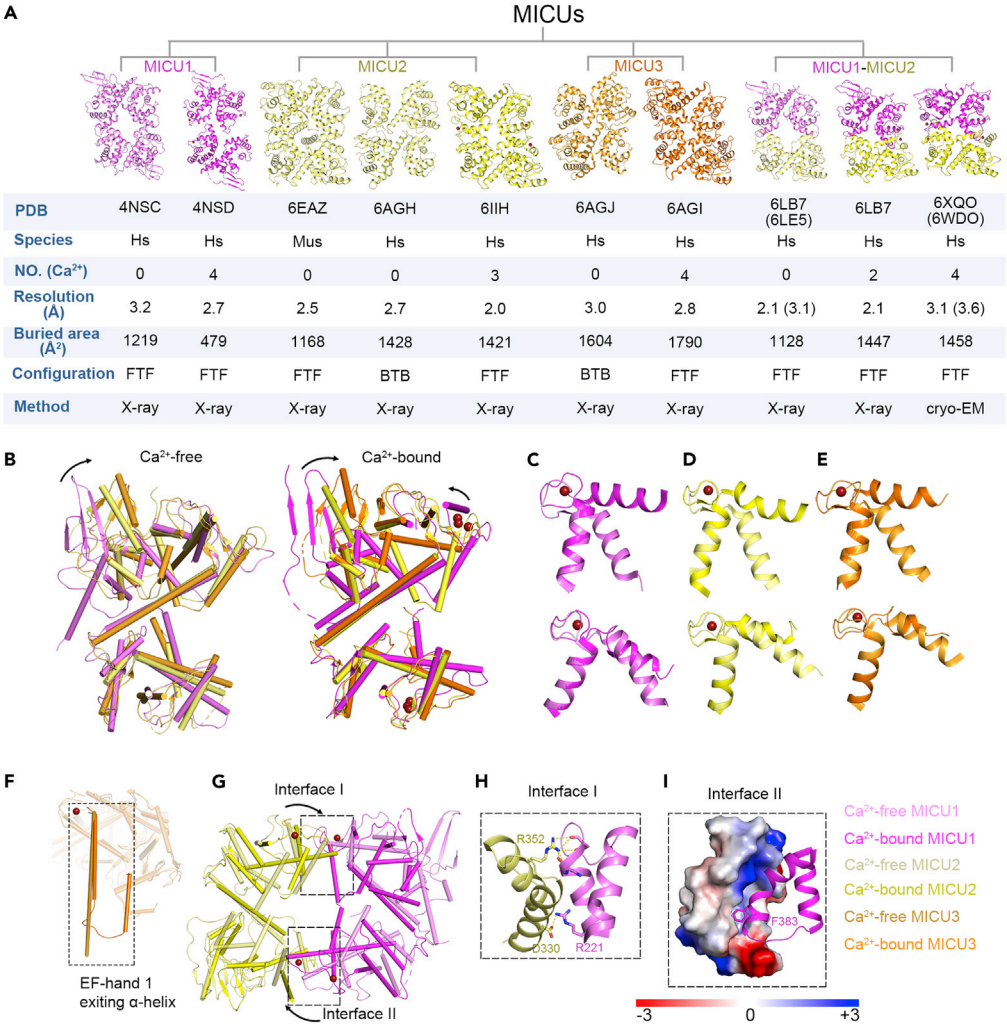

PDB	4NSC	4NSD	6EAZ	6AGH	6IIH	6AGJ	6AGI	6LB7 (6LE5)	6LB7	6XQO (6WDO)
Species	Hs	Hs	Mus	Hs	Hs	Hs	Hs	Hs	Hs	Hs
NO. (Ca^{2+})	0	4	0	0	3	0	4	0	2	4
Resolution (Å)	3.2	2.7	2.5	2.7	2.0	3.0	2.8	2.1 (3.1)	2.1	3.1 (3.6)
Buried area (Å^2)	1219	479	1168	1428	1421	1604	1790	1128	1447	1458
Configuration	FTF	FTF	FTF	BTB	FTF	BTB	FTF	FTF	FTF	FTF
Method	X-ray	X-ray	X-ray	X-ray	X-ray	X-ray	X-ray	X-ray	X-ray	cryo-EM

Figure 2. Structures of MICU homodimers and MICU1-MICU2 heterodimers

(A) Structures of MICU homodimers and MICU1-MICU2 heterodimers with relevant properties. FTF, face-to-face; BTB, back-to-back; Hs, *Homo sapiens*; Mus, mouse.

(B) Structural alignments of MICU1 and MICU2 in both the Ca^{2+}-free (left) and Ca^{2+}-bound (right) states. The movement directions of conformational shifts are indicated by arrows.

(C–E) Structural alignments of Ca^{2+}-free and Ca^{2+}-bound EF-hand 1 (top) and EF-hand 2 (bottom) in MICU1 (C), MICU2 (D), and MICU3 (E).

(F) Structural alignment of EF-hand 1 exiting α-helices in the MICU3 Ca^{2+}-free and Ca^{2+}-bound forms. The exiting α-helices are displayed as long helices in the *apo* state, whereas they are broken into two short helices in the *holo* state.

(G) Structural alignment of Ca^{2+}-free and Ca^{2+}-bound MICU1-MICU2 heterodimers. Interaction interfaces I and II and the movement of the conformational changes are indicated by dotted boxes and arrows, respectively.

(H) Close-up view of Ca^{2+}-free MICU1-MICU2 electrostatic interface I. The crucial residues are shown in stick representation.

(I) Electrostatic surface potential of Ca^{2+}-bound MICU1-MICU2 hydrophobic interface II. The crucial residues are presented in stick representation. The gradient shown is from −3 (acidic, red) to +3 (basic, blue) kT/e.

configurational transformation and elicit functional regulation of mitochondrial Ca^{2+} uptake. Deletion of the MICU1 C-helix resulted in a misadjusted threshold and impaired uniporter activity, illuminating the critical roles of the C-helix (Kamer and Mootha, 2014; Wang et al., 2014). MICU1 enhances the interaction with MCU in the absence of Ca^{2+}, thereby inhibiting Ca^{2+} uptake and disassociating from MCU upon Ca^{2+} coordination to activate the ion pore (Petrungaro et al., 2015; Phillips et al., 2019). In fact, the MICU1 homodimer can function as a gatekeeper and cooperative activator under corresponding conditions independent of MICU2 (Kamer and Mootha, 2014; Payne et al., 2017; Wang et al., 2014).

Three MICU2 structures have been reported, revealing similar structural folds but large differences in assembly patterns. Ca^{2+}-bound MICU2 adopts a face-to-face configuration with an antiparallel mode, whereas the assembly patterns of Ca^{2+}-free structures are controversial (Figure 2A) (Kamer et al., 2019; Wu et al., 2019; Xing et al., 2019). Xing et al. proposed that Ca^{2+}-free human MICU2 and MICU3 structures have back-to-back configurations, whereas the Ca^{2+}-bound MICU3 structure adopts the face-to-face assembly mode (Figure 2A) (Xing et al., 2019). These authors considered MICU2 and MICU3 paralogs to possess the same dimer arrangements opposite to MICU1, likely reflecting the different functional roles of MICU1 (*i.e.*, inhibition of MICU2 and MICU3 *vs.* activation of MICU1) (Xing et al., 2019). Kamer et al. considered that the mouse Ca^{2+}-free MICU2 structure adopts the face-to-face assembly mode, which is the same configuration as MICU1 and Ca^{2+}-bound MICU2 (Figure 2A) (Kamer et al., 2019). Despite the different packing patterns, the interactions observed in MICU1 and MICU3 homodimer structures are generally similar, featuring electrostatic and hydrophobic interactions in the Ca^{2+}-free and Ca^{2+}-bound forms, respectively. The differences in packing are influenced by the selection of the smallest asymmetric unit in the crystallographic lattice. Indeed, the opposite configurations can also be found in all MICU structures. Therefore, the question of which packing arrangement is the most reasonable or relevant emerges. The Ca^{2+}-bound MICU2 packing pattern is indisputable since the interaction of the Ca^{2+}-bound MICU2 homodimer occurs through the EF-hand 1 motifs, which are located in the interaction interface in the face-to-face antiparallel packing mode, making structural sense (Wu et al., 2019). In contrast, the interaction sites of Ca^{2+}-free MICU2 homodimers are controversial, making it difficult to determine the packing arrangements (Wu et al., 2019; Xing et al., 2019). Similar to the C-helix of MICU1, the rigid helix of MICU2 plays a vital role in maintaining the normal threshold under resting conditions (Kamer et al., 2019). To date, a back-to-back configuration has been observed in the tetrameric MICU1-MICU2 complex and is the most likely preferred configuration (as further elaborated in the following) (Fan et al., 2020; Wang et al., 2020c; Zhuo et al., 2020). However, the possibility of the other packing configuration cannot be excluded.

MICU1/2/3 are homologous MCU modulators, but their functions are nonredundant, which is consistent with the conformational differences among their structures. MICU2 structures are more similar to MICU3 but show large conformational discrepancies in the N-lobe compared with MICU1 (Figure 2B) (Wu et al., 2019; Xing et al., 2019). These structural differences dictate the specific functions of each MICU, as exemplified by the fact that exchanging the N-lobes between MICU1 and MICU2 was found to switch their roles (Xing et al., 2019). MICU1/2/3 possess two canonical EF-hands, but the two EF-hand helices undergo different conformational changes upon Ca^{2+} binding. The α-helices of EF-hand 1 are rearranged from an antiparallel mode to an approximately perpendicular configuration upon Ca^{2+} binding, whereas EF-hand 2 exhibits minimal conformational changes between the two forms (Figures 2C–2E) (Wang et al., 2014; Wu et al., 2019; Xing et al., 2019). Despite displaying different structural changes, each EF-hand adopts the typical pentagonal bipyramid geometry with seven Ca^{2+} coordination sites (Wang et al., 2014; Wu et al., 2019). Strikingly, each EF-hand is indispensable and dictates the functions of MICU1/2/3 because compromising the EF-hands caused MCU to remain in the inhibition state (Kamer and Mootha, 2014; Payne et al., 2017). Moreover, other divalent metal ions can bind EF-hands but cannot be coordinated in the same way as Ca^{2+}, resulting in an *apo*-like state of EF-hands (Grabarek, 2011; Senguen and Grabarek, 2012). Thus, the conformational changes (from the off to the on state) in the EF-hands induced by Ca^{2+} constitute an indispensable condition for activating the ion pore (Kamer et al., 2018). Additionally, the exiting α-helix of EF-hand 1 in Ca^{2+}-free MICU3 is longer than that in MICU1/2, but it bends into a U-shaped structure upon Ca^{2+} binding (Figure 2F). This feature was not observed in MICU1/2. This specific conformational change is attributed to α-helix instability because it contains a potential coiled-coil structure in the middle; however, the implication of this structural property remains elusive.

Structures of the MICU1-MICU2 heterodimer

MICU1 and MICU2 form a tightly associated heterodimer to dictate the mitochondrial Ca^{2+} uptake threshold under resting conditions. It is difficult to separate one from the other in individual functional investigations owing to the tight relationship between MICU1 and MICU2. Thus, considering MICU1-MICU2 as a whole is an effective strategy for research on mitochondrial Ca^{2+} uptake mechanisms. An earlier report indicated that MICU1 interacts with MICU2 through a cysteine residue in each C-terminus by forming a disulfide bond in cells mediated by the oxidoreductase Mia40 (Patron et al., 2014; Petrungaro et al., 2015). However, extensive subsequent experimental evidence demonstrated that MICU1 and MICU2 could form a stable heterodimer in the absence of disulfide *in vitro* (Kamer et al., 2017; Li et al., 2016; Wu et al., 2019). Recently, MICU1-MICU2 heterodimer structures were solved by X-ray crystallography, revealing a face-to-face antiparallel assembly (Park et al., 2020; Wu et al., 2020). To date, three different heterodimer MICU1-MICU2 structures have been documented: (1) Ca^{2+}-free (Park et al., 2020; Wu et al., 2020), (2) Ca^{2+}_{part}-bound (partially Ca^{2+}-bound, Ca^{2+} is bound to only

two of the four Ca^{2+}-binding sites) (Wu et al., 2020), and (3) Ca^{2+}-bound structures (Fan et al., 2020; Wang et al., 2020b, 2020c). The superimposed structures of Ca^{2+}-free and Ca^{2+}-bound MICU1-MICU2 heterodimers demonstrate that Ca^{2+}-bound structures are more compact than the *apo* form (Figure 2G). Ca^{2+} stabilizes the MICU1-MICU2 complex, which is reflected not only in the structure but also by size exclusion chromatography (SEC) and isothermal titration calorimetry (ITC) experiments (Kamer et al., 2017; Wu et al., 2019). All three types of structures contain two interaction interfaces. Interface I mainly features electrostatic interactions in the Ca^{2+}-free form, whereas interface II is characterized mainly by hydrophobic interactions in the Ca^{2+}-bound form (Figures 2H and 2I) (Park et al., 2020; Wu et al., 2020). Furthermore, partially Ca^{2+}-bound MICU1-MICU2 features the interface characteristics of both the Ca^{2+}-free and Ca^{2+}-bound forms in one structure, which very likely represents the transition state between *apo* and *holo* and illuminates the process of conformational changes.

The establishment of the Ca^{2+} uptake threshold by MICU1-MICU2 depends on their EF-hands or, more precisely, on their affinity for Ca^{2+} (Kamer et al., 2017). Strikingly, the Ca^{2+} affinities of the MICU1 homodimer and MICU1-MICU2 heterodimer closely resemble the thresholds observed in MICU2 knockout cells (MICU1 homodimer acts as a gatekeeper) and wild-type cells (MICU1-MICU2 heterodimer acts as a gatekeeper), respectively (Kamer et al., 2017). Therefore, Ca^{2+} affinities correspond to the mitochondrial Ca^{2+} uptake threshold under corresponding conditions. Based on the findings described previously, the activation process of mitochondrial Ca^{2+} uptake can be described as the process of a door opening in which Ca^{2+} is the key, the EF-hands are the lock, the Ca^{2+}-binding affinity is the ability to open the door, the MICU1-MICU2 heterodimer is the gatekeeper, and the conformational changes are the turning force required to open the door. When $[Ca^{2+}]_c$ exceeds the threshold (gain privilege), Ca^{2+} ions bind in the EF-hands (open locks) to trigger conformational changes in MICU1-MICU2 (the driving force for opening the door), resulting in dissociation of the heterodimer from MCU to activate the channel.

Recently, two small molecules, MCUi4 and MCUi11, which bind MICU1, were shown to act as negative regulators of MCU and to decrease mitochondrial Ca^{2+} uptake. However, the regulatory mechanism of these inhibitors remains challenging to examine (Di Marco et al., 2020). As suggested by computational simulations, the compounds could be accommodated comfortably in the middle groove between the two lobes of MICU1, which are adjacent to EF-hand 1 of MICU1 (Di Marco et al., 2020). The binding of Ca^{2+} and the triggering of conformational changes are two elements crucial for activating Ca^{2+} channels; however, neither of the two inhibitors affects Ca^{2+} coordination. Thus, the inhibition of MCU is likely due to the compounds impeding the conformational changes in the MICU1-MICU2 heterodimer. The specific regulatory mechanism of the inhibitors needs further investigation, perhaps through determination of the different conformations of MICU1-inhibitor complex structures.

The conserved polybasic sequence KKKKR (polyK) in MICU1 contributes to the interaction with the acidic C-terminal tail of EMRE (Tsai et al., 2016). Recently, the alkaline groove, which consists of a polyK motif and adjacent helices, was identified as the MICU1-EMRE interaction pocket (Wu et al., 2020). The subsequent EMRE-MCU-MICU1-MICU2 structures show that the EMRE C-terminal tail extends to the alkaline groove despite the lack of an intact tail structure, lending further support to the suggestion that the pocket is the interaction site (Fan et al., 2020; Wang et al., 2020b, 2020c; Zhuo et al., 2020). Importantly, the C-terminal peptide of EMRE was able to compete with endogenous EMRE and reduce the threshold of Ca^{2+} uptake under resting conditions but showed minimal influence on the dynamics of Ca^{2+} conduction in mitochondria, further substantiating the anchoring function of the EMRE C-terminus and the gatekeeper role of MICU1-MICU2 (Wu et al., 2020). Moreover, the MICU1-EMRE interaction is Ca^{2+} dependent and is facilitated in the presence of Ca^{2+} (Wu et al., 2020). However, the MICU1-MCU interaction is weakened under this condition, completely opposite to the MICU1-EMRE interaction (Petrungaro et al., 2015; Phillips et al., 2019; Wu et al., 2020). The fascinating contrast between the two interaction scenarios of MICU1-MCU and MICU1-EMRE is informative for investigating the mechanism of mitochondrial Ca^{2+} uptake, which could power the switching of MICU1-MICU2 inhibition and activation activities.

ARCHITECTURE OF THE UNIPORTER SUPERCOMPLEX

Structures of the MCU-EMRE subcomplex

EMRE is a metazoan-specific subunit that is absolutely required for activating MCU Ca^{2+} uptake in metazoans, as evidenced by the inability of MCU to transport Ca^{2+} in EMRE-deficient cells (Sancak et al., 2013). Thus, the MCU-EMRE complex structure is more informative than the single MCU structure for mechanistic investigations of mitochondrial Ca^{2+} uptake. The MCU-EMRE subcomplex structure has been

characterized by single-particle cryo-EM, revealing a V-shaped dimeric channel assembly pattern with an NTD-mediated interaction (Wang et al., 2019). Four EMRE molecules surround the channel at its periphery with an N-terminal β-hairpin implanted in the fenestration ion cavity (Figures 1C and 1I) (Wang et al., 2019, 2020a). As a result, the β-hairpin of EMRE acts on MCU to promote swelling of the ion cavity, probably enabling the accommodation of more Ca^{2+} to increase the Ca^{2+} uptake efficiency. In addition, the strong interaction between EMRE and MCU provides structural support for the luminal gate in an open state (Wang et al., 2019). Very recently, it was reported that EMRE-dependent luminal gate opening was mediated by the hydrophobic residue cluster within the MCU juxtamembrane domain (Van Keuren et al., 2020). EMRE binding induced hydrophobic residues to move to the fenestration in a hydrophobic environment and increased the diameter of the luminal gate through which Ca^{2+} is conducted (Van Keuren et al., 2020). Moreover, the MCU-EMRE hydrophobic interaction increased the energy barrier of EMRE degradation by mAAA proteases (Konig et al., 2016; Patron et al., 2018; Tsai et al., 2017). Thus, EMRE and MCU supplement each other to ensure mitochondrial Ca^{2+} uptake.

In addition to regulating the luminal gate, EMRE mediates the V-shaped dimerization of the MCU channel, which features a curved transmembrane boundary due to the strong interactions of the N-termini (Figure 1C) (Wang et al., 2019). The curved-membrane dimeric MCU-EMRE assembly pattern presents a new perspective on the Ca^{2+} channel architecture. The MCU-EMRE complex potentially resides on the upward convex IMM (*i.e.*, cristae junction) rather than the downward concave membrane (*i.e.*, cristae membrane) to accommodate its specific curve shape. Considering the IMM (consisting of the IBM and cristae membranes) localization of MCU and EMRE under resting conditions and their migration to the IBM upon agonist stimulation (De La Fuente et al., 2016; Gottschalk et al., 2019), Ca^{2+} stimulates their localization changes. However, is the IBM localization of MCU and EMRE in Ca^{2+}-stimulated cells related to the formation of dimeric channels? Alternatively, does Ca^{2+} regulate dimeric EMRE-MCU channel assembly? Indeed, Ca^{2+} ions have been observed in the dimeric channel structure, although the Ca^{2+} "incentive" hypothesis requires further verification. The structural characterizations of the uniporter holocomplex detailed in the following section provide vital insights into these questions.

Structures of the mitochondrial Ca^{2+} uniporter holocomplex

Multiple uniporter holocomplex (MCU-EMRE-MICU1-MICU2) structures have very recently been reported, revealing their spatial assembly with an unexpected stoichiometry of 4:4:1:1 (Figures 3A and 3B) (Fan et al., 2020; Wang et al., 2020b, 2020c; Zhuo et al., 2020). Strikingly, the supercomplex architecture provides new insights into the MICU1-MICU2 gating process, establishing a framework for understanding the mechanism underlying mitochondrial Ca^{2+} uptake. Similar to the MCU-EMRE structure, the four EMREs in the supercomplex are located at the periphery of the MCU channel and anchor one MICU1-MICU2 heterodimer (Fan et al., 2020; Wang et al., 2020b, 2020c; Zhuo et al., 2020). In the Ca^{2+}-free state, MICU1 covers the channel entrance of the MCU pore with extensive electrostatic interactions to impede Ca^{2+} conduction, whereas MICU2 is located on the side of the channel with minimal interaction with MCU (Figure 3A) (Fan et al., 2020; Wang et al., 2020b, 2020c). In the Ca^{2+}-bound state, the MICU1-MICU2 heterodimer is arranged in a linear heterotetramer configuration with another heterodimer of the dimer channel to unblock the MCU pore (Figure 3B) (Fan et al., 2020; Wang et al., 2020c). The structures in the two states provide straightforward pictures of the closed and open states of the uniporter, which greatly enhanced our structural understanding of the gatekeeping and activation of the MICU1-MICU2 complex.

The Ca^{2+}-free holocomplex structure reveals that MICU1 interacts with MCU via abundant electrostatic interactions contributed by the alkaline domain in MICU1 and the Asp ring in MCU (Fan et al., 2020; Paillard et al., 2018; Phillips et al., 2019; Wang et al., 2020a, 2020b). The C-terminal helices in MICU1-MICU2 display a parallel packing mode with a pair of intermolecular disulfide bonds in the holocomplex, which also help stabilize the MCU-MICU1 interaction (Fan et al., 2020). Moreover, the C-terminal helix in MICU1 exhibits hydrophobic interactions with MCU, further elucidating the experimental results of reduced thresholds under resting conditions and weakened interactions with MCU in C-helix deletion cells (Kamer and Mootha, 2014; Wang et al., 2014). Additionally, it has been reported that MICU1 phosphorylation at the N-terminal region affects the maturation process and destabilizes the MICU1-MICU2 heterodimer, leading to increased $[Ca^{2+}]_m$ under basal conditions (Marchi et al., 2018). Based on the *apo* holocomplex structure, the phosphorylation site is located in the interaction area of MCU-MICU1; thus, the steric and charge effects of the phosphate group probably weaken the MCU-MICU1 interaction under resting conditions, possibly abolishing the gatekeeper function. The C-terminus of MICU1 can also be methylated by protein

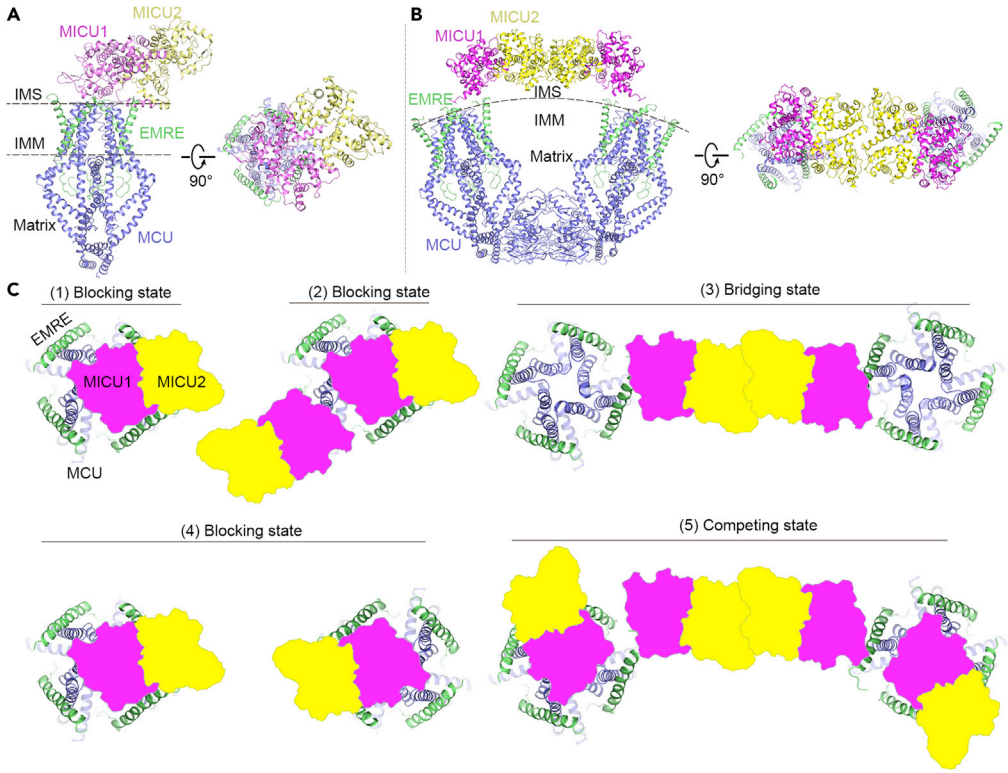

Figure 3. Structures of Ca^{2+}-free and Ca^{2+}-bound uniporter supercomplexes

(A) Side (left) and top (right) views of the Ca^{2+}-free MCU-EMRE-MICU1-MICU2 complex structure.

(B) Side (left) and top (right) views of the Ca^{2+}-bound MCU-EMRE-MICU1-MICU2 dimeric channel complex structure.

(C) Five types of MCU-EMRE-MICU1-MICU2 structural assembly under Ca^{2+}-free conditions. (1) Predominant blocking assembly. The MICU1-MICU2 heterodimer blocks the center of the monomeric MCU channel. (2) Monomeric MCU channel with two MICU1-MICU2 heterodimers attached, i.e., one blocking the center of the monomeric MCU channel and the other tethered on the periphery of the ion channel. (3) The MICU1-MICU2 heterotetramer bridges the V-shaped dimeric channel without blocking the ion pore, forming an O-shaped uniporter. (4) Two heterodimers block the two central pores of the V-shaped dimeric channel. (5) Competition state of blocking and bridging assemblies. Two heterodimers block the entrance of the channel, and a heterotetramer bridges the V-shaped dimeric channel. The heterotetramer is moved to the margin of the dimeric channel owing to competition by the blocking assembly.

arginine methyltransferase 1 (PRMT1), which has been documented to decrease Ca^{2+} sensitivity and reduce uniporter activity compared with that resulting from unmethylated MICU1 under identical Ca^{2+} stimulation conditions (Madreiter-Sokolowski et al., 2016). Although methylated MICU1 clearly affects Ca^{2+} binding and decreases uniporter activity, the methylation site may strengthen the MCU-MICU1 interaction because the site is located near the MCU-MICU1 interface in the *apo* holocomplex structure, which may be another cause of reduced uniporter activity.

Strikingly, multiple configurations of the uniporter holocomplex were observed in the *apo* state, except for the typical monomeric channel blocking state (Figure 3C, 1). For example, (i) two MICU1-MICU2 heterodimers were recruited in one MCU channel, with one heterodimer anchoring on the top surface of MCU to occlude the ion pore and another tethering to the periphery of the MCU pore (only 2%) (Figure 3C, 2) (Wang et al., 2020b); (ii) MICU1-MICU2 assembled into a heterotetramer to bridge the V-shaped dimeric channel, which is similar to the *holo* form (Figure 3C, 3) (Wang et al., 2020c); (iii) two MICU1-MICU2 heterodimers blocked both centers of the V-shaped dimeric channel (Figure 3C, 4) (Wang et al., 2020c); and (iv) in the most complicated configuration, the competing mode, the MICU1-MICU2 heterotetramer bridged the dimeric channel and two MICU1-MICU2 heterodimers occluded the top entrance of MCU, which represents competition or the transition state of the blocking and bridging assemblies (Figure 3C, 5) (Wang et al., 2020c). However, the nonmainstream assembly patterns account for only a small percentage of cases, which can probably be attributed to conformational heterogeneity in addition to the major occlusion monomeric model.

Notably, another recently determined uniporter structure reveals an O-shaped ring within the MICU1-MICU2 heterotetramer bridging the dimeric channel in a presumably Ca^{2+}-free form resulting from EGTA (EGTA is a specific calcium ion chelator)-containing purification conditions (Zhuo et al., 2020). Surprisingly, this structure exhibits the same assembly pattern as Ca^{2+}-bound structures (Fan et al., 2020; Wang et al., 2020c). Superimposing this heterodimer with the determinate *apo* and *holo* states shows that its conformation is similar to the *holo* form but displays a large conformational discrepancy with the *apo* form. In this case, although the Ca^{2+}-chelating agent EGTA was added during the purification process, the features of the EF-hand conformations and interaction interfaces were similar to those of the Ca^{2+}-bound form. This bewildering result was also observed in MICU2 and MICU1-MICU2 structures, in which indisputable Ca^{2+} electron density was observed, even though 2 mM EGTA was added as a chelating agent under crystallization conditions (Wu et al., 2019, 2020). Assuming that the resulting nonocclusion model in the *apo* form was established, how can the inhibition phenomenon under basal conditions be explained? How can the strong MCU-MICU1 interaction in the absence of Ca^{2+} be explained? Coincidentally, multiple configurations in *apo* models observed in another report also contain this assembly (Wang et al., 2020c); however, the resolution is too low to permit a detailed and meaningful structure alignment analysis.

Taken together, these results indicate that the MICU1-MICU2 gatekeeper occludes the entrance of the MCU pore to inhibit Ca^{2+} transport under resting conditions and migrates to the periphery of the channel to activate MCU under stimulation conditions. The sophisticated regulation in metazoan MCU reveals the precise and multilevel modulation required in higher organisms to ensure rapid and effective responses to signals. Furthermore, these supercomplex structures provide a framework for understanding mitochondrial Ca^{2+} transport activity and inspire the proposed regulatory mechanism models, including the Ca^{2+}-dependent interaction switch model, EMRE-dependent recognition probability model, and lever regulation model. These models demonstrate the conceivable dynamic process of Ca^{2+}-dependent MICU1-MICU2 activation and the possible MICU1-MICU2-dependent gating mechanism, as elaborated in the following.

PROPOSED STRUCTURAL MECHANISTIC MODELS

Interaction switch model

The uniporter architectures offer many valuable hints for investigating the regulatory mechanism of the MICU1-MICU2 heterodimer. However, the role of EMRE in anchoring MICU1-MICU2 is less clear. EMRE was regarded as the bridging component connecting MICU1 with MCU in an earlier report (Sancak et al., 2013) and was considered to possess dual functions, including the activation of MCU and maintenance of the MICU1-MICU2 association with Ca^{2+} channels (Tsai et al., 2016). Thus far, it is accepted that EMRE and MCU can interact with MICU1 under opposite Ca^{2+} conditions. MICU1 strengthens the interactions with MCU or EMRE in the absence or presence of Ca^{2+}, respectively (Petrungaro et al., 2015; Phillips et al., 2019; Wu et al., 2020). Thus, we proposed a working model of an interaction switch in which MICU1 associates with MCU under resting conditions to inhibit Ca^{2+} uptake and is converted to interact with EMRE upon increased $[Ca^{2+}]_c$ to activate the channels (Wu et al., 2020). Moreover, the interaction switches between MCU-MICU1 and EMRE-MICU1 reconcile the transformation of the two opposite functions, i.e., gatekeeping and activation, and help rationalize the Ca^{2+} signal transduction pathway of mitochondrial Ca^{2+} uptake.

Recognition probability model

Although EMRE is undoubtedly necessary for metazoan mitochondrial Ca^{2+} uptake, the stoichiometric ratio of MCU and EMRE remains debatable. EMRE-MCU and uniporter holocomplex structures demonstrate that one channel possesses four EMRE molecules symmetrically arranged around the pore. In another recent report, variable numbers of EMREs in the MCU channel ranging from one to four were observed (Payne et al., 2020). The gatekeeping function was strengthened as the number of EMRE molecules increased, and two EMREs were considered appropriate in the physiological state to maintain the normal threshold (Payne et al., 2020). Considering the supercomplex structures and the finding of variable numbers of EMREs, we proposed a regulatory model that helps reconcile the apparent confusion arising from the multiple EMREs and the single MICU1-MICU2 heterodimer. As a tetramer, the MCU entrance plane displays fourfold symmetry, permitting the MICU1-MICU2 heterodimer to interact in any of four orientations with the assistance of EMREs. More available interacting positions as a result of the increasing number of EMREs are coupled with the higher probability of recognition and interaction between MICU1-MICU2 and MCU, as well as the higher gatekeeping efficiency (Figure 4) (Wu et al., 2020). Thus, EMRE likely plays a guiding role in helping identify the appropriate binding position of MICU1. Although this model seems to reconcile the mismatching number of MICU1-MICU2 and EMRE perfectly, some questions remain. For instance, how is the most appropriate orientation of the MICU1-

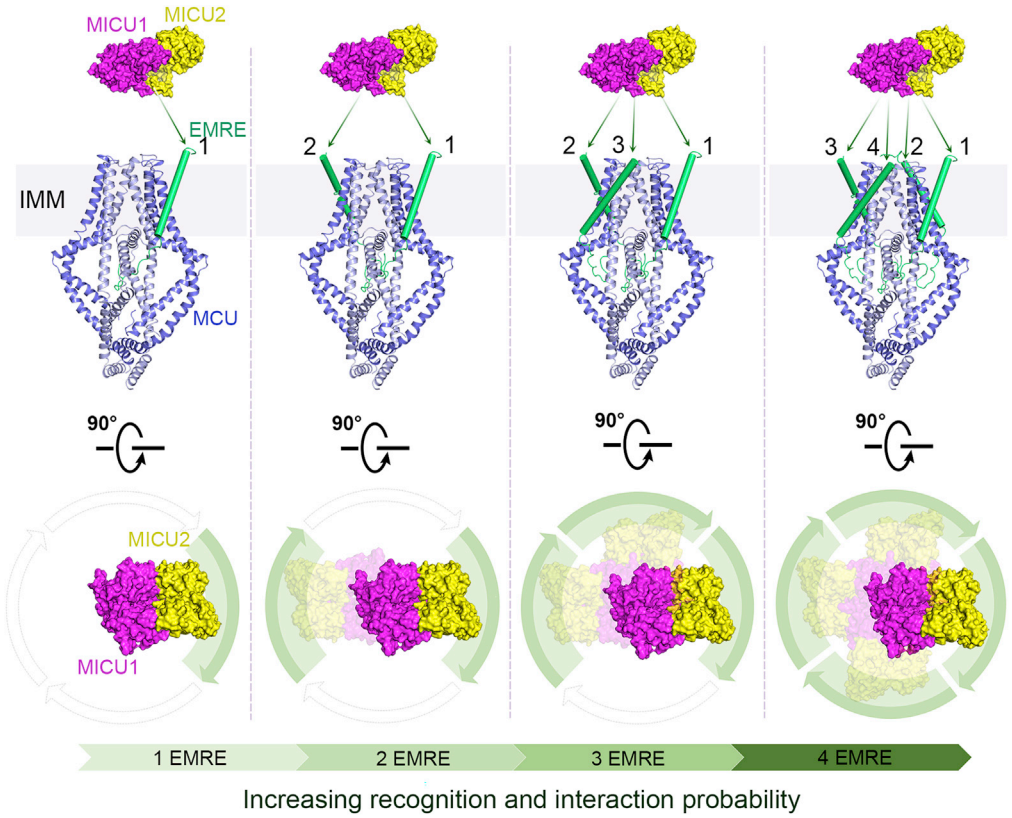

Figure 4. Probability model of the MICU1-MICU2 heterodimer recognizing and interacting with the channel

This model reconciles the apparent disagreement between variable EMREs and a single MICU1-MICU2 regulator in one channel. The entrance plane of the MCU channel possesses fourfold symmetry and allows MICU1 blocking in any of the four orientations. EMREs act as guiders helping MICU1 recognize and interact with the channel. As the number of EMREs increases from one to four, the recognition probability also increases from one-fourth to one, resulting in enhanced gatekeeping activity and efficiency.

MICU2 heterodimer determined given the fourfold symmetry? Are the four structurally equivalent orientations also functionally equivalent? Why do organisms evolve redundant EMRE molecules if two molecules appear to be sufficient for uniporter activities? Although the recognition/interaction probability model is plausible, our knowledge of this model is currently restricted given the limited existing experimental data.

Lever regulation model

We currently have structural information regarding the beginning and ending states of the mitochondrial Ca^{2+} uptake process owing to powerful cryo-EM techniques. However, the intermediate state(s) and transition process remain elusive. The MICU1-MICU2 heterodimer saturated with Ca^{2+} exhibited a slightly bent conformation that is markedly more compact than the *apo* form (Fan et al., 2020; Wang et al., 2020b, 2020c; Wu et al., 2020). If the heterodimer still maintains the obstruction assembly mode upon Ca^{2+} binding, conformational changes in MICU1-MICU2 could lead to insertion of the hydrophilic region of MICU2 into the membrane, a conformation that does not appear to satisfy thermodynamic requirements (Wang et al., 2020b, 2020c). An interesting lever regulation model was proposed in which EMRE and the helix (CC2a) in the MCU coiled-coil domain act as two levers (Zhuo et al., 2020). At the first level, EMRE is attached to the fenestration ion cavity and MICU1-MICU2 heterodimer (Figure 5). At the second level, CC2a is attached to TM2 of MCU and EMRE β-hairpins (Figure 5) (Zhuo et al., 2020). When Ca^{2+} ions are coordinated by EF-hands, both heterodimers are pried from the top of the pore by the levers and move away from the channel entrance site as a result of rearrangement to a linear heterotetrameric configuration (Figure 5). In addition, the interaction switches between MCU-MICU1 and EMRE-MICU1 probably provide a driving force for this movement in response to Ca^{2+} signaling. This double-level model provides a new perspective on the dynamic process of Ca^{2+} uptake.

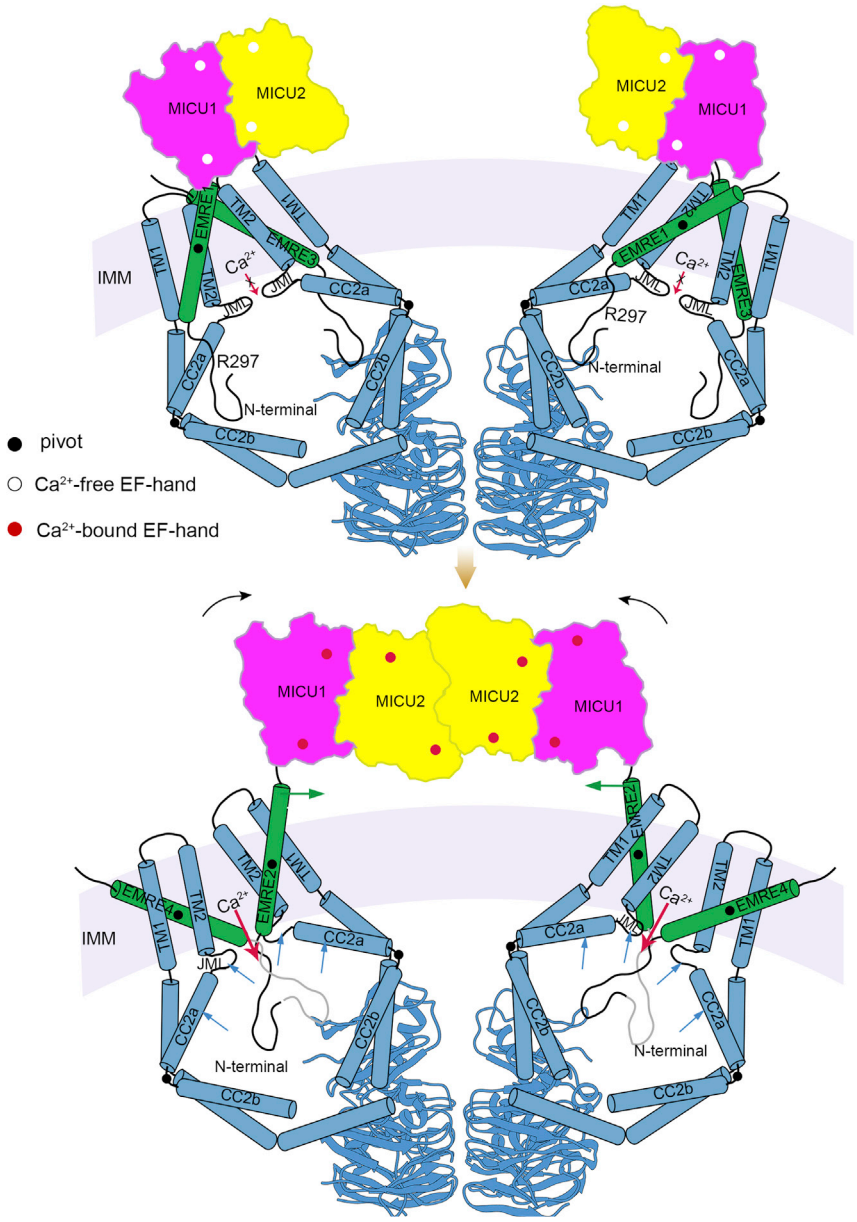

Figure 5. Lever model of MICU1-MICU2 heterodimers depicting the transition process between the blocked and unblocked states

EMRE and the CC2a helix are the first and second levers with a pivot on the EMRE and the middle linker of CC2a and the following broken helix (CC2b), respectively. In the first level, EMRE is attached to the fenestration ion cavity and MICU1-MICU2 heterodimer via the N-terminal β-hairpin and C-terminal tail, respectively. In the second level, CC2a is attached to TM2 of MCU and EMRE β-hairpins via the N-termini and Arg297 in the CC2a helix, respectively. When $[Ca^{2+}]_c$ is increased, the MICU1-MICU2 heterodimer disassociates from MCU and moves via lever actions, reassembling in a heterotetrameric linear configuration. The pivot and acting forces of the levers are shown as black dots and correspondingly colored arrows.

CONCLUSIONS AND PERSPECTIVES

Here, we described the multicomponent structures of the mitochondrial uniporter and, by integration with functional experimental results, we proposed and rationalized Ca^{2+} uptake and regulatory mechanisms. Various MCU structures support the parallel Ca^{2+} permeation mechanism while revealing differences in structural domains and channel assemblies across species (Baradaran et al., 2018; Fan et al.,

2018; Nguyen et al., 2018; Wang et al., 2019, 2020a; Yoo et al., 2018). The Ca^{2+}-free and Ca^{2+}-bound modulatory subunit MICU1-3 structures reveal large structural discrepancies between MICU1 and MICU2/3 and provide insights into gatekeeping regulatory models; however, the assembly patterns remain controversial (Kamer et al., 2019; Wang et al., 2014; Wu et al., 2019; Xing et al., 2019). Three different MICU1-MICU2 structural states demonstrate the conformational transition from the *apo* to the *holo* state, clarifying the structural basis between gatekeeping and activation (Park et al., 2020; Wang et al., 2020b; Wu et al., 2020). On the one hand, EMRE regulates the Ca^{2+} transportation luminal gate by maintaining the opening of the juxtamembrane channel; on the other hand, EMRE triggers the dimerization of MCU to form the V-shaped dimeric channel, providing a new perspective on the Ca^{2+} channel structure (Wang et al., 2019). Ca^{2+}-free and Ca^{2+}-bound MCU-EMRE-MICU1-MICU2 uniporter holocomplex structures reveal gatekeeping and activation mechanisms through regulation by MICU1-MICU2. The MICU1-MICU2 heterodimer blocks the channel entrance to inhibit Ca^{2+} permeation in the *apo* state but moves toward the periphery of the channel to remove occlusion and rearranges to a linear heterotetramer bridging the V-shaped dimeric channel in the *holo* state (Fan et al., 2020; Wang et al., 2020c). These structural characterizations explain the Ca^{2+} conduction and gatekeeping activity of the regulators, establishing a structural framework for understanding the functional mechanism of mitochondrial Ca^{2+} uptake.

The interaction switch mode between MICU1-MCU and MICU1-EMRE provides convincing insights into the mechanism of transitioning between gatekeeping and activation, and the probability and lever models offer additional and thought-provoking possibilities regarding more detailed regulatory features (Wu et al., 2020; Zhuo et al., 2020). Notably, the probability and lever models are proposals based on the integration of available structural and functional analyses and need further investigation. Several regulatory models illuminate the mechanisms of Ca^{2+} uptake in mitochondria from different perspectives. Although functional and structural characterizations have made remarkable progress in recent years, several questions regarding the regulatory mechanisms remain unanswered. Currently, we still do not clearly understand the endogenous stoichiometric ratio between EMRE and MCU. The MICU1-MICU2 heterodimer is removed to the side of the pore when MCU is activated. How does MCU re-recruit the heterodimer as the gatekeeper under resting conditions, given that they are far apart? What is the significance of the uniplex dimer because it is not necessary for uniporter Ca^{2+} uptake? Do the four EF-hands in the MICU1-MICU2 heterodimer coordinate Ca^{2+} simultaneously or sequentially? If the latter, is there a hierarchical or multilevel mechanism by which MICU1-MICU2 modulates Ca^{2+} uptake? Further studies are needed to address these fundamental questions. In addition to its essential role in cellular processes, the mitochondrial Ca^{2+} uniporter has been closely linked to several human diseases, including neuromuscular disease and neurodevelopmental disorders (Lewis-Smith et al., 2016; Logan et al., 2014; Shamseldin et al., 2017). It is hoped that with increasing understanding of the structural basis of mitochondrial Ca^{2+} uptake, future research may begin to focus on developing potential therapeutic interventions.

ACKNOWLEDGMENTS

This work was supported by grants from the National Natural Science Foundation of China (No. 21773014) and Natural Sciences and Engineering Research Council of Canada (No. RGPIN-2018-04427).

AUTHOR CONTRIBUTIONS

Z. J. and J. Z. suggested the proposal and supervised the work. W. W. drafted the manuscript and prepared the figures. All the authors discussed the results and commented on the manuscript.

DECLARATION OF INTERESTS

The authors declare that they have no conflicts of interest with the contents of this article.

REFERENCES

Ahuja, M., and Muallem, S. (2014). The gatekeepers of mitochondrial calcium influx: MICU1 and MICU2. EMBO Rep. *15*, 205–206. https://doi.org/10.1002/embr.201438446.

Ashrafi, G., de Juan-Sanz, J., Farrell, R.J., and Ryan, T.A. (2020). Molecular tuning of the axonal mitochondrial Ca(2+) uniporter ensures metabolic flexibility of Neurotransmission. Neuron *105*, 678–687.e5. https://doi.org/10.1016/j.neuron.2019.11.020.

Balaban, R.S. (2009). The role of Ca(2+) signaling in the coordination of mitochondrial ATP production with cardiac work. Biochim. Biophys. Acta *1787*, 1334–1341. https://doi.org/10.1016/j.bbabio.2009.05.011.

Baradaran, R., Wang, C., Siliciano, A.F., and Long, S.B. (2018). Cryo-EM structures of fungal and metazoan mitochondrial calcium uniporters. Nature *559*, 580–584. https://doi.org/10.1038/s41586-018-0331-8.

Barsukova, A., Komarov, A., Hajnoczky, G., Bernardi, P., Bourdette, D., and Forte, M. (2011). Activation of the mitochondrial permeability transition pore modulates Ca2+ responses to physiological stimuli in adult neurons. Eur. J. Neurosci. *33*, 831–842. https://doi.org/10.1111/j.1460-9568.2010.07576.x.

Baughman, J.M., Perocchi, F., Girgis, H.S., Plovanich, M., Belcher-Timme, C.A., Sancak, Y., Bao, X.R., Strittmatter, L., Goldberger, O., Bogorad, R.L., et al. (2011). Integrative genomics identifies MCU as an essential component of the mitochondrial calcium uniporter. Nature *476*, 341–345. https://doi.org/10.1038/nature10234.

Bick, A.G., Calvo, S.E., and Mootha, V.K. (2012). Evolutionary diversity of the mitochondrial calcium uniporter. Science *336*, 886. https://doi.org/10.1126/science.1214977.

Boyman, L., and Lederer, W.J. (2020). How the mitochondrial calcium uniporter complex (MCUcx) works COMMENT. Proc. Natl. Acad. Sci. U S A *117*, 22634–22636. https://doi.org/10.1073/pnas.2015886117.

Cao, C., Wang, S., Cui, T., Su, X.C., and Chou, J.J. (2017). Ion and inhibitor binding of the double-ring ion selectivity filter of the mitochondrial calcium uniporter. Proc. Natl. Acad. Sci. U S A *114*, E2846–E2851. https://doi.org/10.1073/pnas.1620316114.

Chaudhuri, D., Sancak, Y., Mootha, V.K., and Clapham, D.E. (2013). MCU encodes the pore conducting mitochondrial calcium currents. Elife *2*, e00704. https://doi.org/10.7554/eLife.00704.

Crompton, M., Kunzi, M., and Carafoli, E. (1977). The calcium-induced and sodium-induced effluxes of calcium from heart mitochondria. Evidence for a sodium-calcium carrier. Eur. J. Biochem. *79*, 549–558. https://doi.org/10.1111/j.1432-1033.1977.tb11839.x.

Csordas, G., Golenar, T., Seifert, E.L., Kamer, K.J., Sancak, Y., Perocchi, F., Moffat, C., Weaver, D., Perez, S.F., Bogorad, R., et al. (2013). MICU1 controls both the threshold and cooperative activation of the mitochondrial Ca(2)(+) uniporter. Cell Metab. *17*, 976–987. https://doi.org/10.1016/j.cmet.2013.04.020.

Csordas, G., Thomas, A.P., and Hajnoczky, G. (1999). Quasi-synaptic calcium signal transmission between endoplasmic reticulum and mitochondria. EMBO J. *18*, 96–108.

Csordas, G., Varnai, P., Golenar, T., Roy, S., Purkins, G., Schneider, T.G., Balla, T., and Hajnoczky, G. (2010). Imaging Interorganelle contacts and local calcium dynamics at the ER-mitochondrial interface. Mol. Cell *39*, 121–132.

De La Fuente, S., Fernandez-Sanz, C., Vail, C., Agra, E.J., Holmstrom, K., Sun, J., Mishra, J., Williams, D., Finkel, T., Murphy, E., et al. (2016). Strategic positioning and biased activity of the mitochondrial calcium uniporter in cardiac muscle. J. Biol. Chem. *291*, 23343–23362. https://doi.org/10.1074/jbc.M116.755496.

De Stefani, D., Raffaello, A., Teardo, E., Szabo, I., and Rizzuto, R. (2011). A forty-kilodalton protein of the inner membrane is the mitochondrial calcium uniporter. Nature *476*, 336–340. https://doi.org/10.1038/nature10230.

Denton, R.M. (2009). Regulation of mitochondrial dehydrogenases by calcium ions. Biochim. Biophys. Acta *1787*, 1309–1316. https://doi.org/10.1016/j.bbabio.2009.01.005.

Di Marco, G., Vallese, F., Jourde, B., Bergsdorf, C., Sturlese, M., De Mario, A., Techer-Etienne, V., Haasen, D., Oberhauser, B., Schleeger, S., et al. (2020). A high-throughput screening identifies MICU1 targeting compounds. Cell Rep. *30*, 2321–2331 e2326. https://doi.org/10.1016/j.celrep.2020.01.081.

Docampo, R., Vercesi, A.E., and Huang, G. (2014). Mitochondrial calcium transport in trypanosomes. Mol. Biochem. Parasitol. *196*, 108–116. https://doi.org/10.1016/j.molbiopara.2014.09.001.

Dong, Z., Shanmughapriya, S., Tomar, D., Siddiqui, N., Lynch, S., Nemani, N., Breves, S.L., Zhang, X., Tripathi, A., Palaniappan, P., et al. (2017). Mitochondrial Ca(2+) uniporter is a mitochondrial luminal redox sensor that augments MCU channel activity. Mol. Cell *65*, 1014–1028 e1017. https://doi.org/10.1016/j.molcel.2017.01.032.

Drago, I., Pizzo, P., and Pozzan, T. (2011). After half a century mitochondrial calcium in- and efflux machineries reveal themselves. EMBO J. *30*, 4119–4125. https://doi.org/10.1038/emboj.2011.337.

Duchen, M.R., Verkhratsky, A., and Muallem, S. (2008). Mitochondria and calcium in health and disease. Cell Calcium *44*, 1–5. https://doi.org/10.1016/j.ceca.2008.02.001.

Elrod, J.W., Wong, R., Mishra, S., Vagnozzi, R.J., Sakthievel, B., Goonasekera, S.A., Karch, J., Gabel, S., Farber, J., Force, T., et al. (2010). Cyclophilin D controls mitochondrial pore-dependent Ca(2+) exchange, metabolic flexibility, and propensity for heart failure in mice. J. Clin. Invest. *120*, 3680–3687. https://doi.org/10.1172/JCI43171.

Fan, C., Fan, M., Orlando, B.J., Fastman, N.M., Zhang, J., Xu, Y., Chambers, M.G., Xu, X., Perry, K., Liao, M., and Feng, L. (2018). X-ray and cryo-EM structures of the mitochondrial calcium uniporter. Nature *559*, 575–579. https://doi.org/10.1038/s41586-018-0330-9.

Fan, M., Zhang, J., Tsai, C.W., Orlando, B.J., Rodriguez, M., Xu, Y., Liao, M., Tsai, M.F., and Feng, L. (2020). Structure and mechanism of the mitochondrial Ca(2+) uniporter holocomplex. Nature *582*, 129–133. https://doi.org/10.1038/s41586-020-2309-6.

Foskett, J.K., and Madesh, M. (2014). Regulation of the mitochondrial Ca(2+) uniporter by MICU1 and MICU2. Biochem. Biophys. Res. Commun. *449*, 377–383. https://doi.org/10.1016/j.bbrc.2014.04.146.

Giacomello, M., Drago, I., Bortolozzi, M., Scorzeto, M., Gianelle, A., Pizzo, P., and Pozzan, T. (2010). Ca2+ hot spots on the mitochondrial surface are generated by Ca2+ mobilization from stores, but not by activation of store-operated Ca2+ channels. Mol. Cell *38*, 280–290.

Gottschalk, B., Klec, C., Leitinger, G., Bernhart, E., Rost, R., Bischof, H., Madreiter-Sokolowski, C.T., Radulovic, S., Eroglu, E., Sattler, W., et al. (2019). MICU1 controls cristae junction and spatially anchors mitochondrial Ca(2+) uniporter complex. Nat. Commun. *10*, 3732. https://doi.org/10.1038/s41467-019-11692-x.

Grabarek, Z. (2011). Insights into modulation of calcium signaling by magnesium in calmodulin, troponin C and related EF-hand proteins. Biochim. Biophys. Acta *1813*, 913–921. https://doi.org/10.1016/j.bbamcr.2011.01.017.

Graier, W.F., Frieden, M., and Malli, R. (2007). Mitochondria and Ca(2+) signaling: old guests, new functions. Pflugers Arch. *455*, 375–396. https://doi.org/10.1007/s00424-007-0296-1.

Gunter, T.E., and Pfeiffer, D.R. (1990). Mechanisms by which mitochondria transport calcium. Am. J. Physiol. *258*, C755–C786. https://doi.org/10.1152/ajpcell.1990.258.5.C755.

Hiller, S., and Wagner, G. (2009). The role of solution NMR in the structure determinations of VDAC-1 and other membrane proteins. Curr. Opin. Struct. Biol. *19*, 396–401.

Huang, C., and Kalodimos, C.G. (2017). Structures of large protein complexes determined by nuclear magnetic resonance spectroscopy. Annu. Rev. Biophys. *46*, 317–336. https://doi.org/10.1146/annurev-biophys-070816-033701.

Ichas, F., Jouaville, L.S., and Mazat, J.P. (1997). Mitochondria are excitable organelles capable of generating and conveying electrical and calcium signals. Cell *89*, 1145–1153. https://doi.org/10.1016/s0092-8674(00)80301-3.

Jiang, D., Zhao, L., and Clapham, D.E. (2009). Genome-wide RNAi screen identifies Letm1 as a mitochondrial Ca2+/H+ antiporter. Science *326*, 144–147. https://doi.org/10.1126/science.1175145.

Kamer, K.J., Grabarek, Z., and Mootha, V.K. (2017). High-affinity cooperative Ca(2+) binding by MICU1-MICU2 serves as an on-off switch for the uniporter. EMBO Rep. *18*, 1397–1411. https://doi.org/10.15252/embr.201643748.

Kamer, K.J., Jiang, W., Kaushik, V.K., Mootha, V.K., and Grabarek, Z. (2019). Crystal structure of MICU2 and comparison with MICU1 reveal insights into the uniporter gating mechanism. Proc. Natl. Acad. Sci. U S A *116*, 3546–3555. https://doi.org/10.1073/pnas.1817759116.

Kamer, K.J., and Mootha, V.K. (2014). MICU1 and MICU2 play nonredundant roles in the regulation of the mitochondrial calcium uniporter. EMBO Rep. *15*, 299–307. https://doi.org/10.1002/embr.201337946.

Kamer, K.J., and Mootha, V.K. (2015). The molecular era of the mitochondrial calcium uniporter. Nat. Rev. Mol. Cell Biol. *16*, 545–553. https://doi.org/10.1038/nrm4039.

Kamer, K.J., Sancak, Y., Fomina, Y., Meisel, J.D., Chaudhuri, D., Grabarek, Z., and Mootha, V.K. (2018). MICU1 imparts the mitochondrial uniporter with the ability to discriminate between Ca(2+) and Mn(2+). Proc. Natl. Acad. Sci. U S A *115*, E7960–E7969. https://doi.org/10.1073/pnas.1807811115.

Kirichok, Y., Krapivinsky, G., and Clapham, D.E. (2004). The mitochondrial calcium uniporter is a highly selective ion channel. Nature *427*, 360–364. https://doi.org/10.1038/nature02246.

Konig, T., Troder, S.E., Bakka, K., Korwitz, A., Richter-Dennerlein, R., Lampe, P.A., Patron, M., Muhlmeister, M., Guerrero-Castillo, S., Brandt, U., et al. (2016). The m-AAA protease associated with neurodegeneration limits MCU activity in mitochondria. Mol. Cell *64*, 148–162. https://doi.org/10.1016/j.molcel.2016.08.020.

Kovacs-Bogdan, E., Sancak, Y., Kamer, K.J., Plovanich, M., Jambhekar, A., Huber, R.J., Myre, M.A., Blower, M.D., and Mootha, V.K. (2014). Reconstitution of the mitochondrial calcium uniporter in yeast. Proc. Natl. Acad. Sci. U S A *111*, 8985–8990. https://doi.org/10.1073/pnas.1400514111.

Lambert, J.P., Luongo, T.S., Tomar, D., Jadiya, P., Gao, E., Zhang, X., Lucchese, A.M., Kolmetzky, D.W., Shah, N.S., and Elrod, J.W. (2019). MCUB regulates the molecular composition of the mitochondrial calcium uniporter channel to limit mitochondrial calcium overload during stress. Circulation *140*, 1720–1733. https://doi.org/10.1161/CIRCULATIONAHA.118.037968.

Lander, N., Chiurillo, M.A., Bertolini, M.S., Docampo, R., and Vercesi, A.E. (2018). The mitochondrial calcium uniporter complex in trypanosomes. Cell Biol. Int. *42*, 656–663. https://doi.org/10.1002/cbin.10928.

Lee, S.K., Shanmughapriya, S., Mok, M.C.Y., Dong, Z., Tomar, D., Carvalho, E., Rajan, S., Junop, M.S., Madesh, M., and Stathopulos, P.B. (2016). Structural insights into mitochondrial calcium uniporter regulation by divalent cations. Cell Chem. Biol. *23*, 1157–1169. https://doi.org/10.1016/j.chembiol.2016.07.012.

Lee, Y., Min, C.K., Kim, T.G., Song, H.K., Lim, Y., Kim, D., Shin, K., Kang, M., Kang, J.Y., Youn, H.S., et al. (2015). Structure and function of the N-terminal domain of the human mitochondrial calcium uniporter. EMBO Rep. *16*, 1318–1333. https://doi.org/10.15252/embr.201540436.

Lewis-Smith, D., Kamer, K.J., Griffin, H., Childs, A.M., Pysden, K., Titov, D., Duff, J., Pyle, A., Taylor, R.W., Yu-Wai-Man, P., et al. (2016). Homozygous deletion in MICU1 presenting with fatigue and lethargy in childhood. Neurol. Genet. *2*, e59. https://doi.org/10.1212/NXG.0000000000000059.

Li, D., Wu, W., Pei, H., Wei, Q., Yang, Q., Zheng, J., and Jia, Z. (2016). Expression and preliminary characterization of human MICU2. Biol. Open *5*, 962–969. https://doi.org/10.1242/bio.018572.

Logan, C.V., Szabadkai, G., Sharpe, J.A., Parry, D.A., Torelli, S., Childs, A.M., Kriek, M., Phadke, R., Johnson, C.A., Roberts, N.Y., et al. (2014). Loss-of-function mutations in MICU1 cause a brain and muscle disorder linked to primary alterations in mitochondrial calcium signaling. Nat. Genet. *46*, 188–193. https://doi.org/10.1038/ng.2851.

Madreiter-Sokolowski, C.T., Klec, C., Parichatikanond, W., Stryeck, S., Gottschalk, B., Pulido, S., Rost, R., Eroglu, E., Hofmann, N.A., Bondarenko, A.I., et al. (2016). PRMT1-mediated methylation of MICU1 determines the UCP2/3 dependency of mitochondrial Ca(2+) uptake in immortalized cells. Nat. Commun. *7*, 12897. https://doi.org/10.1038/ncomms12897.

Mallilankaraman, K., Cardenas, C., Doonan, P.J., Chandramoorthy, H.C., Irrinki, K.M., Golenar, T., Csordas, G., Madireddi, P., Yang, J., Muller, M., et al. (2012a). MCUR1 is an essential component of mitochondrial Ca2+ uptake that regulates cellular metabolism. Nat. Cell Biol. *14*, 1336–1343. https://doi.org/10.1038/ncb2622.

Mallilankaraman, K., Doonan, P., Cardenas, C., Chandramoorthy, H.C., Muller, M., Miller, R., Hoffman, N.E., Gandhirajan, R.K., Molgo, J., Birnbaum, M.J., et al. (2012b). MICU1 is an essential gatekeeper for MCU-mediated mitochondrial Ca(2+) uptake that regulates cell survival. Cell *151*, 630–644. https://doi.org/10.1016/j.cell.2012.10.011.

Marchi, S., Corricelli, M., Branchini, A., Vitto, V.A.M., Missiroli, S., Morciano, G., Perrone, M., Ferrarese, M., Giorgi, C., Pinotti, M., et al. (2018). Akt-mediated phosphorylation of MICU1 regulates mitochondrial Ca(2+) levels and tumor growth. EMBO J. https://doi.org/10.15252/embj.201899435.

Marchi, S., and Pinton, P. (2014). The mitochondrial calcium uniporter complex: molecular components, structure and physiopathological implications. J. Physiol. *592*, 829–839. https://doi.org/10.1113/jphysiol.2013.268235.

Martell, J.D., Deerinck, T.J., Sancak, Y., Poulos, T.L., Mootha, V.K., Sosinsky, G.E., Ellisman, M.H., and Ting, A.Y. (2012). Engineered ascorbate peroxidase as a genetically encoded reporter for electron microscopy. Nat. Biotechnol. *30*, 1143.

Mishra, J., Jhun, B.S., Hurst, S., J, O.U., Csordas, G., and Sheu, S.S. (2017). The mitochondrial Ca(2+) uniporter: structure, function, and pharmacology. Handb. Exp. Pharmacol. *240*, 129–156. https://doi.org/10.1007/164_2017_1.

Murgia, M., and Rizzuto, R. (2015). Molecular diversity and pleiotropic role of the mitochondrial calcium uniporter. Cell Calcium *58*, 11–17. https://doi.org/10.1016/j.ceca.2014.11.001.

Nguyen, N.X., Armache, J.P., Lee, C., Yang, Y., Zeng, W., Mootha, V.K., Cheng, Y., Bai, X.C., and Jiang, Y. (2018). Cryo-EM structure of a fungal mitochondrial calcium uniporter. Nature *559*, 570–574. https://doi.org/10.1038/s41586-018-0333-6.

Nicholls, D.G. (2005). Mitochondria and calcium signaling. Cell Calcium *38*, 311–317. https://doi.org/10.1016/j.ceca.2005.06.011.

O'Rourke, B. (2007). Mitochondrial ion channels. Annu. Rev. Physiol. *69*, 19–49. https://doi.org/10.1146/annurev.physiol.69.031905.163804.

O-Uchi, J., Jhun, B.S., Xu, S.C., Hurst, S., Raffaello, A., Liu, X.Y., Yi, B., Zhang, H.L., Gross, P., Mishra, J., et al. (2014). Adrenergic signaling regulates mitochondrial Ca2+ uptake through pyk2-dependent tyrosine phosphorylation of the mitochondrial Ca2+ uniporter. Antioxid. Redox Sig. *21*, 863–879.

Orrenius, S., Zhivotovsky, B., and Nicotera, P. (2003). Regulation of cell death: the calcium-apoptosis link. Nat. Rev. Mol. Cell Biol. *4*, 552–565. https://doi.org/10.1038/nrm1150.

Oxenoid, K., Dong, Y., Cao, C., Cui, T., Sancak, Y., Markhard, A.L., Grabarek, Z., Kong, L., Liu, Z., Ouyang, B., et al. (2016). Architecture of the mitochondrial calcium uniporter. Nature *533*, 269–273. https://doi.org/10.1038/nature17656.

Paillard, M., Csordas, G., Huang, K.T., Varnai, P., Joseph, S.K., and Hajnoczky, G. (2018). MICU1 interacts with the D-ring of the MCU pore to control its Ca(2+) flux and sensitivity to Ru360. Mol. Cell *72*, 778–785 e773. https://doi.org/10.1016/j.molcel.2018.09.008.

Palty, R., Ohana, E., Hershfinkel, M., Volokita, M., Elgazar, V., Beharier, O., Silverman, W.F., Argaman, M., and Sekler, I. (2004). Lithium-calcium exchange is mediated by a distinct potassium-independent sodium-calcium exchanger. J. Biol. Chem. *279*, 25234–25240.

Palty, R., Silverman, W.F., Hershfinkel, M., Caporale, T., Sensi, S.L., Parnis, J., Nolte, C., Fishman, D., Shoshan-Barmatz, V., Herrmann, S., et al. (2010). NCLX is an essential component of mitochondrial Na+/Ca2+ exchange. Proc. Natl. Acad. Sci. U S A *107*, 436–441.

Park, J., Lee, Y., Park, T., Kang, J.Y., Mun, S.A., Jin, M., Yang, J., and Eom, S.H. (2020). Structure of the MICU1–MICU2 heterodimer provides insights into the gatekeeping threshold shift. IUCrJ *7*, 355–365. https://doi.org/10.1107/s2052252520001840.

Patergnani, S., Suski, J.M., Agnoletto, C., Bononi, A., Bonora, M., De Marchi, E., Giorgi, C., Marchi, S., Missiroli, S., Poletti, F., et al. (2011). Calcium signaling around mitochondria associated membranes (MAMs). Cell Commun. Signal. *9*, 19. https://doi.org/10.1186/1478-811X-9-19.

Patron, M., Checchetto, V., Raffaello, A., Teardo, E., Vecellio Reane, D., Mantoan, M., Granatiero, V., Szabo, I., De Stefani, D., and Rizzuto, R. (2014). MICU1 and MICU2 finely tune the mitochondrial Ca2+ uniporter by exerting opposite effects on MCU activity. Mol. Cell *53*, 726–737. https://doi.org/10.1016/j.molcel.2014.01.013.

Patron, M., Granatiero, V., Espino, J., Rizzuto, R., and De Stefani, D. (2019). MICU3 is a tissue-specific enhancer of mitochondrial calcium uptake. Cell Death Differ. *26*, 179–195. https://doi.org/10.1038/s41418-018-0113-8.

Patron, M., Sprenger, H.G., and Langer, T. (2018). m-AAA proteases, mitochondrial calcium homeostasis and neurodegeneration. Cell Res *28*, 296–306. https://doi.org/10.1038/cr.2018.17.

Paupe, V., Prudent, J., Dassa, E.P., Rendon, O.Z., and Shoubridge, E.A. (2015). CCDC90A (MCUR1) is a cytochrome c oxidase assembly factor and not a regulator of the mitochondrial calcium uniporter. Cell Metab. *21*, 109–116. https://doi.org/10.1016/j.cmet.2014.12.004.

Payne, R., Hoff, H., Roskowski, A., and Foskett, J.K. (2017). MICU2 restricts spatial crosstalk between InsP3R and MCU channels by regulating threshold and gain of MICU1-mediated inhibition and activation of MCU. Cell Rep. *21*, 3141–3154. https://doi.org/10.1016/j.celrep.2017.11.064.

Payne, R., Li, C., and Foskett, J.K. (2020). Variable assembly of EMRE and MCU creates functional channels with distinct gatekeeping profiles. iScience *23*, 101037. https://doi.org/10.1016/j.isci.2020.101037.

Perocchi, F., Gohil, V.M., Girgis, H.S., Bao, X.R., McCombs, J.E., Palmer, A.E., and Mootha, V.K. (2010). MICU1 encodes a mitochondrial EF

hand protein required for Ca(2+) uptake. Nature *467*, 291–296. https://doi.org/10.1038/nature09358.

Petrungaro, C., Zimmermann, K.M., Kuttner, V., Fischer, M., Dengjel, J., Bogeski, I., and Riemer, J. (2015). The Ca(2+)-dependent release of the mia40-induced MICU1-MICU2 dimer from MCU regulates mitochondrial Ca(2+) uptake. Cell Metab. *22*, 721–733. https://doi.org/10.1016/j.cmet.2015.08.019.

Phillips, C.B., Tsai, C.W., and Tsai, M.F. (2019). The conserved aspartate ring of MCU mediates MICU1 binding and regulation in the mitochondrial calcium uniporter complex. Elife *8*. https://doi.org/10.7554/eLife.41112.

Pittis, A.A., Goh, V., Cebrian-Serrano, A., Wettmarshausen, J., Perocchi, F., and Gabaldon, T. (2020). Discovery of EMRE in fungi resolves the true evolutionary history of the mitochondrial calcium uniporter. Nat. Commun. *11*, 4031. https://doi.org/10.1038/s41467-020-17705-4.

Plovanich, M., Bogorad, R.L., Sancak, Y., Kamer, K.J., Strittmatter, L., Li, A.A., Girgis, H.S., Kuchimanchi, S., De Groot, J., Speciner, L., et al. (2013). MICU2, a paralog of MICU1, resides within the mitochondrial uniporter complex to regulate calcium handling. PLoS One *8*, e55785. https://doi.org/10.1371/journal.pone.0055785.

Popovych, N., Tzeng, S.R., Tonelli, M., Ebright, R.H., and Kalodimos, C.G. (2009). Structural basis for cAMP-mediated allosteric control of the catabolite activator protein. Proc. Natl. Acad. Sci. U S A *106*, 6927–6932. https://doi.org/10.1073/pnas.0900595106.

Raffaello, A., De Stefani, D., Sabbadin, D., Teardo, E., Merli, G., Picard, A., Checchetto, V., Moro, S., Szabo, I., and Rizzuto, R. (2013). The mitochondrial calcium uniporter is a multimer that can include a dominant-negative pore-forming subunit. EMBO J. *32*, 2362–2376. https://doi.org/10.1038/emboj.2013.157.

Rasola, A., and Bernardi, P. (2007). The mitochondrial permeability transition pore and its involvement in cell death and in disease pathogenesis. Apoptosis *12*, 815–833.

Rizzuto, R., De Stefani, D., Raffaello, A., and Mammucari, C. (2012). Mitochondria as sensors and regulators of calcium signalling. Nat. Rev. Mol. Cell Biol. *13*, 566–578. https://doi.org/10.1038/nrm3412.

Rizzuto, R., Pinton, P., Carrington, W., Fay, F.S., Fogarty, K.E., Lifshitz, L.M., Tuft, R.A., and Pozzan, T. (1998). Close contacts with the endoplasmic reticulum as determinants of mitochondrial Ca2+ responses. Science *280*, 1763–1766. https://doi.org/10.1126/science.280.5370.1763.

Sancak, Y., Markhard, A.L., Kitami, T., Kovacs-Bogdan, E., Kamer, K.J., Udeshi, N.D., Carr, S.A., Chaudhuri, D., Clapham, D.E., Li, A.A., et al. (2013). EMRE is an essential component of the mitochondrial calcium uniporter complex. Science *342*, 1379–1382. https://doi.org/10.1126/science.1242993.

Senguen, F.T., and Grabarek, Z. (2012). X-ray structures of magnesium and manganese complexes with the N-terminal domain of calmodulin: insights into the mechanism and specificity of metal ion binding to an EF-hand. Biochemistry *51*, 6182–6194. https://doi.org/10.1021/bi300698h.

Shamseldin, H.E., Alasmari, A., Salih, M.A., Samman, M.M., Mian, S.A., Alshidi, T., Ibrahim, N., Hashem, M., Faqeih, E., Al-Mohanna, F., and Alkuraya, F.S. (2017). A null mutation in MICU2 causes abnormal mitochondrial calcium homeostasis and a severe neurodevelopmental disorder. Brain *140*, 2806–2813. https://doi.org/10.1093/brain/awx237.

Tomar, D., Dong, Z., Shanmughapriya, S., Koch, D.A., Thomas, T., Hoffman, N.E., Timbalia, S.A., Goldman, S.J., Breves, S.L., Corbally, D.P., et al. (2016). MCUR1 is a scaffold factor for the MCU complex function and promotes mitochondrial bioenergetics. Cell Rep. *15*, 1673–1685. https://doi.org/10.1016/j.celrep.2016.04.050.

Tsai, C.W., Wu, Y., Pao, P.C., Phillips, C.B., Williams, C., Miller, C., Ranaghan, M., and Tsai, M.F. (2017). Proteolytic control of the mitochondrial calcium uniporter complex. Proc. Natl. Acad. Sci. U S A *114*, 4388–4393. https://doi.org/10.1073/pnas.1702938114.

Tsai, M.F., Jiang, D., Zhao, L., Clapham, D., and Miller, C. (2014). Functional reconstitution of the mitochondrial Ca2+/H+ antiporter Letm1. J. Gen. Physiol. *143*, 67–73. https://doi.org/10.1085/jgp.201311096.

Tsai, M.F., Phillips, C.B., Ranaghan, M., Tsai, C.W., Wu, Y., Willliams, C., and Miller, C. (2016). Dual functions of a small regulatory subunit in the mitochondrial calcium uniporter complex. Elife *5*. https://doi.org/10.7554/eLife.15545.

Tugarinov, V., Choy, W.Y., Orekhov, V.Y., and Kay, L.E. (2005). Solution NMR-derived global fold of a monomeric 82-kDa enzyme. Proc. Natl. Acad. Sci. U S A *102*, 622–627.

Tzeng, S.R., Pai, M.T., and Kalodimos, C.G. (2012). NMR studies of large protein systems. Methods Mol. Biol. *831*, 133–140. https://doi.org/10.1007/978-1-61779-480-3_8.

Vais, H., Payne, R., Paudel, U., Li, C., and Foskett, J.K. (2020). Coupled transmembrane mechanisms control MCU-mediated mitochondrial Ca(2+) uptake. Proc. Natl. Acad. Sci. U S A *117*, 21731–21739. https://doi.org/10.1073/pnas.2005976117.

Van Keuren, A.M., Tsai, C.W., Balderas, E., Rodriguez, M.X., Chaudhuri, D., and Tsai, M.F. (2020). Mechanisms of EMRE-dependent MCU opening in the mitochondrial calcium uniporter complex. Cell Rep. *33*, 108486. https://doi.org/10.1016/j.celrep.2020.108486.

Vecellio Reane, D., Vallese, F., Checchetto, V., Acquasaliente, L., Butera, G., De Filippis, V., Szabo, I., Zanotti, G., Rizzuto, R., and Raffaello, A. (2016). A MICU1 splice variant confers high sensitivity to the mitochondrial Ca(2+) uptake machinery of skeletal muscle. Mol. Cell *64*, 760–773. https://doi.org/10.1016/j.molcel.2016.10.001.

Wang, L., Yang, X., Li, S., Wang, Z., Liu, Y., Feng, J., Zhu, Y., and Shen, Y. (2014). Structural and mechanistic insights into MICU1 regulation of mitochondrial calcium uptake. EMBO J. *33*, 594–604. https://doi.org/10.1002/embj.201386523.

Wang, C., Baradaran, R., and Long, S.B. (2020a). Structure and reconstitution of a MCU-EMRE mitochondrial Ca(2+) uniporter complex. J. Mol. Biol. https://doi.org/10.1016/j.jmb.2020.08.013.

Wang, C., Jacewicz, A., Delgado, B.D., Baradaran, R., and Long, S.B. (2020b). Structures reveal gatekeeping of the mitochondrial Ca(2+) uniporter by MICU1-MICU2. Elife *9*. https://doi.org/10.7554/eLife.59991.

Wang, Y., Han, Y., She, J., Nguyen, N.X., Mootha, V.K., Bai, X.C., and Jiang, Y. (2020c). Structural insights into the Ca(2+)-dependent gating of the human mitochondrial calcium uniporter. Elife *9*. https://doi.org/10.7554/eLife.60513.

Wang, Y., Nguyen, N.X., She, J., Zeng, W., Yang, Y., Bai, X.C., and Jiang, Y. (2019). Structural mechanism of EMRE-dependent gating of the human mitochondrial calcium uniporter. Cell *177*, 1252–1261 e1213. https://doi.org/10.1016/j.cell.2019.03.050.

Wu, W., Shen, Q., Lei, Z., Qiu, Z., Li, D., Pei, H., Zheng, J., and Jia, Z. (2019). The crystal structure of MICU2 provides insight into Ca(2+) binding and MICU1-MICU2 heterodimer formation. EMBO Rep. *20*, e47488. https://doi.org/10.15252/embr.201847488.

Wu, W., Shen, Q., Zhang, R., Qiu, Z., Wang, Y., Zheng, J., and Jia, Z. (2020). The structure of the MICU1-MICU2 complex unveils the regulation of the mitochondrial calcium uniporter. EMBO J. *39*, e104285. https://doi.org/10.15252/embj.2019104285.

Xing, Y., Wang, M., Wang, J., Nie, Z., Wu, G., Yang, X., and Shen, Y. (2019). Dimerization of MICU proteins controls Ca(2+) influx through the mitochondrial Ca(2+) uniporter. Cell Rep. *26*, 1203–1212 e1204. https://doi.org/10.1016/j.celrep.2019.01.022.

Yoo, J., Wu, M., Yin, Y., Herzik, M.A., Jr., Lander, G.C., and Lee, S.Y. (2018). Cryo-EM structure of a mitochondrial calcium uniporter. Science *361*, 506–511. https://doi.org/10.1126/science.aar4056.

Yuan, Y., Cao, C., Wen, M., Li, M., Dong, Y., Wu, L., Wu, J., Cui, T., Li, D., Chou, J.J., and OuYang, B. (2020). Structural characterization of the N-terminal domain of the Dictyostelium discoideum mitochondrial calcium uniporter. ACS Omega *5*, 6452–6460. https://doi.org/10.1021/acsomega.9b04045.

Zhuo, W., Zhou, H., Guo, R., Yi, J., Zhang, L., Yu, L., Sui, Y., Zeng, W., Wang, P., and Yang, M. (2020). Structure of intact human MCU supercomplex with the auxiliary MICU subunits. Protein Cell. https://doi.org/10.1007/s13238-020-00776-w.